

Dr. Wolfgang Hering

Bachelor thesis

**Simulation of set into operation experiments of the Karlsruhe
Sodium Laboratory**

Author:

Juan Serrano Llabrés

Karlsruhe, 1st. March 2017

Supervisors:

Dr. W. Hering

Prof. Dr. Fernando Hernández Jiménez



Institut für Fusions- und Reaktortechnik
Bereich: Anlagenentwicklung, Systemdynamik und Sicherheit (ASS)
Leiter: Dr. Wolfgang Hering

Bachelor Thesis

Work Program

Datum: Montag, 27. März 2017
Bearbeiter/in:
Telefon: 0721 60 82 2556
Fax:
E-Mail: wolfgang.hering@kit.edu
Unser Zeichen:

Title: Simulation of set into operation experiments of the Karlsruhe Sodium Laboratory and comparison with results of existing pre-calculations

At KIT-INR the KARlsruhe SODium LABORatory (KASOLA) has been erected to boost the (www.inr.kit.edu/258.php) liquid metal technology for concentrating solar power (CSP) plants. The facility will be extended next year by a thermal storage (FlexStor) and a small sodium receiver with a small mirror system on the roof of the KASOLA tower (see picture right side).

In a first step several set into operation test and experiments have to be performed to assure facility reliability and performance. Also some experiments on dynamic facility behaviour have been pre-determined by several codes as part of the 7th EU Framework Programme. Introduction into TRACE helps to support test preparation. TRACE is used to become acquainted with the KASOLA facility and to learn and understand responses of actions, an important advantage for proposing new experiments.

In that context the following BA/MA thesis is defined:

- a) KASOLA Technology and control system
- b) Test section heater and instrumentation
- c) TRACE code with KASOLA facility model (Training simulator, the input deck is already developed, only parameter changes are necessary)
- d) Elaboration of tests in cooperation with KASOLA team.
- e) Qualification of proposed test by pre-test analyses using TRACE
- f) Analyses of experimental data and elaboration of sensor quality.
- g) Comparison of experimental results with available pre-test calculations performed during recent EU-Collaboration.
- h) Analyses with respect of possible improvements.
- i) Documentation and presentation of results.



ABSTRACT

The purpose of this bachelor thesis is the simulation and analysis of loss of coolant accidents for KASOLA, a facility built at the KIT research centre, in the Institute for Neutron Physics and Reactor Technology (INR), and created for the analysis of sodium as working fluid in nuclear and solar thermal power plants.

In this work, three different experiments for loss of coolant will be modelled and simulated using the TRACE code with the help of the SNAP interface. The model of KASOLA is obtained from previous projects and improvements and changes have been done. In this way, throughout the simulations, the evolution of the flow of sodium out of the facility can be studied in order to evaluate the damage of the accident and to elaborate prevention and safety measures.

With the available components of the software, the different scenarios have been modelled and simulated. They consist on a small break in the piping system, a larger one that takes the flow of sodium through the thermal insulation into consideration and a small break of an instrumentation pipe.

Finally, the results are monitored with the AptPlot software and the amount of lost sodium is for each scenario studied. These are only theoretical tests, and lack of experimental validation. However, the contribution of this project is important at the time of facing accidents or setbacks.

RESUMEN

El presente trabajo de fin de grado tiene por objetivo la simulación y análisis de accidentes de pérdidas de refrigerante en KASOLA, una instalación construida en el centro de investigación de la universidad Karlsruhe Institute of Technology, en el Instituto de Física de Neutrones y Técnica de Reactores (INR), y creada para el estudio del sodio como fluido de trabajo en centrales nucleares y solares térmicas.

En este trabajo, se modelarán tres casos de pérdida de refrigerante distintos utilizando el código TRACE mediante la interfaz SNAP. El modelo de KASOLA se obtiene de proyectos previos y el cual será modificado y optimizado para llevar a cabo simulaciones que permitirán analizar la evolución del flujo de sodio fuera de la instalación. El interés del trabajo reside en la posibilidad de predecir daños en accidentes y elaborar medidas de seguridad y prevención más fiables en el futuro.

Con los componentes disponibles en el software empleado, los distintos escenarios se han modelado y simulado. Ellos consisten en una rotura pequeña en el sistema principal de tuberías, una rotura grande donde se tiene en cuenta el flujo a través del material aislante de la instalación y una rotura pequeña en una tubería de instrumentación.

Finalmente los resultados serán monitorizados con el software AptPlot y la cantidad de sodio perdido será estudiado para cada caso. Se trata, pues, de pruebas teóricas carentes de validación experimental. Sin embargo, la contribución de este proyecto es importante a la hora de afrontar accidentes y contratiempos ya que plantea consideraciones a tener en cuenta en la operación de KASOLA.

ACKNOWLEDGEMENTS

First and foremost I have to thank my research supervisors, Mr. Wolfgang Hering (KIT) and Mr. Fernando Hernández (UC3M), who since the beginning have encouraged me to elaborate and decide the contents and the path of this project. Thank you for your motivation and support and for showing me your fascination for physics and engineering.

I would also like to show gratitude to the beginners of everything, my parents Irene and Javier. Thank you for showing me to watch the reality and to admire it.

Throughout my life I have always shown astonishment for the fact that we can know and understand. In the immensity of universe there is an individual who is the human being and is able to know. The will for knowing always more and the passion for my career has pushed me to where I stand now. I also want to thank my friends, specially the one who once told me *"If we really want to be amazed and touched because the Reality is there, because it exists, we need the capability for staring it in silence. This spectacle, however, makes me to ask more questions because the more I discover, the more I am amazed"*.

I am grateful to the University Carlos III of Madrid, my home university, and the Karlsruhe Institute of Technology for allowing the possibility of writing this thesis in Germany. I finally want to thank my institute companions during the writing of this thesis, to the more experienced and the new ones. Thank you for such a welcome.

CONTENTS

Abstract	i
Resumen	ii
Acknowledgements	iii
Contents	iv
Figures	vii
Tables	ix
Nomenclature	xi
Abbreviations	xii
1 Introduction	1
1.1 Context and motivation of the project.....	1
1.2 Objectives of the project	2
2 Sodium in power conversion systems	3
2.1 Material properties of sodium.....	3
2.2 Sodium-cooled fast reactors	3
2.3 Sodium in solar thermal power plants	5
3 Karlsruhe Sodium Laboratory	6
3.1 Helmholtz Alliance LIMTECH.....	6
3.2 KASOLA overview	6
3.3 Design	8

3.4	Base Loop	9
3.5	Support and safety system	10
3.6	Capabilities	11
4	Numerical Simulation Software	12
4.1	The TRACE code	12
5	Description of the KASOLA TRACE Model	15
5.1	TRACE components for KASOLA	16
5.2	Hydraulic components	17
5.3	Control Blocks	18
6	Simulation and Results	19
6.1	Steady-State simulation	19
6.2	Drainage simulation for small break at the basic loop	20
6.3	Instrumentation pipe break simulation out of the insulation	29
6.4	Large break to the insulation simulation	34
7	Conclusions	44
8	Project expenses estimation	46
8.1	Engineering hours	46
8.2	Project director	46
8.3	Software license acquisition.....	46
8.4	Electronic equipment	47
8.5	General costs	47
8.6	Summary	47

References	48
Appendix	49
A.1 Results for Drainage simulation of KASOLA with 2 and 3 breaks.	49
A.2 Empirical study on the application of correlations for fluxes through porous media.	57

FIGURES

<i>Figure 2.1. Principle of a pool-type sodium-cooled fast reactor.(A Technology Roadmap for Generation IV Nuclear Energy Systems).....</i>	<i>4</i>
<i>Figure 2.2. Scheme of an innovative sodium based conversion system with a secondary molten salt storage system (Conceptual study of central receiver systems with liquid metals).....</i>	<i>5</i>
<i>Figure 3.1. Section of a 3D model of the KASOLA facility</i>	<i>7</i>
<i>Figure 3.2. KASOLA loop inside the containment facility and the underground sodium storage.....</i>	<i>8</i>
<i>Figure 5.1 Detail of the KASOLA model and the hydraulic components.....</i>	<i>15</i>
<i>Figure 6.1. Pressure convergence at the steady state simulation</i>	<i>20</i>
<i>Figure 6.2. Model of KASOLA and Break location.....</i>	<i>21</i>
<i>Figure 6.3. Heat exchanger before renodalization.....</i>	<i>24</i>
<i>Figure 6.4. Heat exchanger after renodalization</i>	<i>24</i>
<i>Figure 6.5. Detail of the mass flow rate of the HX in Drain 3 after the renodalization.....</i>	<i>24</i>
<i>Figure 6.6.Drainage Accumulated mass loss</i>	<i>26</i>
<i>Figure 6.7. Drainage Mass flow rate</i>	<i>26</i>
<i>Figure 6.8. Drainage accumulated mass loss for cases 3 and 4</i>	<i>27</i>
<i>Figure 6.9. Drainage mass flow rate for cases 3 and 4.....</i>	<i>28</i>
<i>Figure 6.10. Instrumentation pipe geometry</i>	<i>30</i>
<i>Figure 6.11. Instrumentation Pipe Accumulated mass loss.....</i>	<i>31</i>
<i>Figure 6.12. Instrumentation Pipe Mass flow rate.....</i>	<i>31</i>
<i>Figure 6.13. Detail of the mass flow rate from cases 1 and 2</i>	<i>32</i>
<i>Figure 6.14. Accumulated mass loss for cases 3 and 4</i>	<i>32</i>
<i>Figure 6.15. Mass flow rate for cases 3 and 4</i>	<i>33</i>
<i>Figure 6.16. Detail of the insulation modeling.....</i>	<i>36</i>
<i>Figure 6.17. Detail of the insulation at the bend modelling.....</i>	<i>36</i>
<i>Figure 6.18. Accumulated Sodium mass flow through Valve 50.....</i>	<i>38</i>
<i>Figure 6.19. Accumulated Sodium mass flow through Break 10.....</i>	<i>38</i>

<i>Figure 6.20. Sodium mass flow rate through Break 10.....</i>	<i>39</i>
<i>Figure 6.21. Total pressure at the break before and after the valve opens.....</i>	<i>39</i>
<i>Figure 6.22. Accumulated sodium mass flow through Valve 50 for cases 3 and 4</i>	<i>40</i>
<i>Figure 6.23. Sodium mass flow rate through Valve 50 for cases 3 and 4.....</i>	<i>41</i>
<i>Figure 6.24. Accumulated sodium mass flow through Break 10 for cases 3 and 4</i>	<i>41</i>
<i>Figure 6.25. Sodium mass flow rate through Break 10 for cases 3 and 4.....</i>	<i>42</i>
<i>Figure 6.26. Detail of the mass flow rate at 6000 seconds for cases 3 and 4.....</i>	<i>42</i>
<i>Figure 0.1. KASOLA model with the 2 positions of the breaks</i>	<i>49</i>
<i>Figure 0.2. Accumulated sodium mass flow through Valve 10</i>	<i>50</i>
<i>Figure 0.3. Sodium mass flow rate through Valve 10</i>	<i>50</i>
<i>Figure 0.4. Accumulated sodium mass flow through Valve 11</i>	<i>51</i>
<i>Figure 0.5. Sodium mass flow rate through Valve 11</i>	<i>51</i>
<i>Figure 0.6. KASOLA model with the 3 positions of the breaks</i>	<i>52</i>
<i>Figure 0.7. . Accumulated sodium mass flow through Valve 10</i>	<i>53</i>
<i>Figure 0.8. Sodium mass flow rate through Valve 10</i>	<i>53</i>
<i>Figure 0.9. Accumulated Sodium mass flow through Valve 11</i>	<i>54</i>
<i>Figure 0.10. Sodium mass flow rate for Valve 11</i>	<i>54</i>
<i>Figure 0.11. Accumulated Sodium mass flow through Valve 61</i>	<i>55</i>
<i>Figure 0.12. Sodium mass flow rate through Valve 61</i>	<i>55</i>
<i>Figure 0.13. Cylindrical tube full with spheres (left) and model of a channel bundle (right).....</i>	<i>57</i>
<i>Figure 0.14. Ergun equation and the two asymptotes related to the Blake-Kozeny and Burke-Plummer equations</i>	<i>59</i>

TABLES

<i>Table 2.1. Properties of sodium and other light metals in simulation conditions...</i>	<i>3</i>
<i>Table 5.1. Geometrical and initial values at each cell for every component. (*)</i>	
<i>The length of the basic loop encloses the drain line, bypass line and HX drain...</i>	<i>18</i>
<i>Table 6.1 Overview of the features of each scenario.....</i>	<i>19</i>
<i>Table 6.2. Valve configuration for each scenario</i>	<i>22</i>
<i>Table 6.3 Initial Conditions of the facility.....</i>	<i>22</i>
<i>Table 6.4. Timestep data table for scenarios 1 and 2.....</i>	<i>25</i>
<i>Table 6.5: Timestep data table for scenarios 3 and 4</i>	<i>25</i>
<i>Table 6.6. Drainage problem final values</i>	<i>28</i>
<i>Table 6.7. Valve configuration for each scenario</i>	<i>29</i>
<i>Table 6.8. Timestep data table for scenarios 1 and 2.....</i>	<i>30</i>
<i>Table 6.9. Timestep data table for scenarios 3 and 4.....</i>	<i>30</i>
<i>Table 6.10. Mass loss and mass flow rate final values (cases 1 and 2)</i>	<i>33</i>
<i>Table 6.11. Mass loss and mass flow rate final values (cases 3 and 4)</i>	<i>34</i>
<i>Table 6.12. Valve configuration for each scenario</i>	<i>35</i>
<i>Table 6.13. Model initial conditions.....</i>	<i>37</i>
<i>Table 6.14. Timestep data table for scenarios 1 and 2.....</i>	<i>37</i>
<i>Table 6.15. Timestep data table for scenarios 3 and 4.....</i>	<i>37</i>
<i>Table 6.16. Total sodium mass loss values for cases 1 and 2.....</i>	<i>40</i>
<i>Table 6.17. Total sodium mass loss values for cases 3 and 4.....</i>	<i>43</i>
<i>Table 0.1. Valve opening configuration for 2 breaks</i>	<i>50</i>
<i>Table 0.2. Total mass lost through Valve 10</i>	<i>51</i>
<i>Table 0.3. Total mass lost through Valve 11</i>	<i>52</i>
<i>Table 0.4. Total mass lost for each scenario</i>	<i>52</i>
<i>Table 0.5. Valve opening configuration for 3 breaks</i>	<i>53</i>
<i>Table 0.6. Total mass lost through Valve 10</i>	<i>56</i>
<i>Table 0.7. Total mass lost through Valve 11</i>	<i>56</i>
<i>Table 0.8. Total mass lost through Valve 61</i>	<i>56</i>
<i>Table 0.9. Total mass lost for each scenario</i>	<i>56</i>

Table 0.10. Obtained values for the friction factor60

NOMENCLATURE

u_i	Velocity at the phase interphase
u_l	Velocity of the liquid phase
u_g	Velocity of the gas phase
α	Gas volume fraction
g	Magnitude of the gravity vector
P	Fluid pressure
Γ	Interfacial mass-transfer rate
ρ_l	Liquid density
ρ_g	Gas density
f_i	Force per unit volume at the interface
f_{wl}	Wall shear force acting on the liquid
f_{wg}	Wall shear force acting on the gas
t	Time
e_l	Internal energy of the liquid phase
e_g	Internal energy of the gas phase
q_{wl}	Heat transfer rate per unit volume from the wall to the liquid phase
q_{wg}	Heat transfer rate per unit volume from the wall to the gas phase
q_{il}	Heat transferred from the interphase to the liquid phase
q_{ig}	Heat transferred from the interphase to the gas phase
q_{al}	Direct heating of the liquid phase
q_{dg}	Direct heating of the gas phase
h'_v	Vapour enthalpy
B_0	Permeability coefficient
μ	Viscosity
ΔP	Pressure difference [Pa]
L	Length of the porous sample [m]
ζ	Friction coefficient
ε	Porosity of the media
D	Hydraulic diameter [m]
ϵ	Roughness [m]

ABBREVIATIONS

ALIP	Annular Linear Induction Pump
AMTEC	Alkali Metal Thermal to Electric Converter
BFS	Backward Facing Step
CFD	Computational Fluid Dynamics
DN	Nominal Pipe Size (fr. <i>diamètre nominal</i>)
FLIP	Flat Linear Induction Pump
HEMCP	Helmholtz Energy Materials Characterization Platform
HX	Heat Exchanger
INR	Institute Institute for Neutron Physics and Reactor Technology
KASOLA	Karlsruhe Sodium Laboratory
KIT	Karlsruhe Institute of Technology
LIMTECH	Helmholtz Alliance on Liquid Metal Technology
MHD	Magneto-hydrodynamic pump
RELAP	Reactor Excursion and Leak Analysis Program
SNAP	Symbolic Nuclear Analysis Package
TRACE	TRAC/RELAP Advanced Computational Engine
USNRC	U.S. Nuclear Regulatory Commission

1 INTRODUCTION

1.1 Context and motivation of the project

In industrialized societies, permanent and reliable electrical energy supply is indispensable. Constant growth of developing countries and the constant raise of world's population make the demand of this kind of energy to increase at significant rate. However, generation of electricity is responsible for most of greenhouse effect gases emissions and this, is an aspect of great concern for the majority of the society. As the effects of the climate change are being observed since several years, the electricity sector plays an important role in the industrial revolution against it. For this reason, research and development in electricity generation is always needed, in order to achieve more efficient power plants, safer and with less or no emissions. Although the contribution from renewable energy sources has grown significantly since the last thirty years, it is important to balance the power sources to cover the actual electricity demand (Energy for the future - The Nuclear Option). For this reason the nuclear energy is still a reasonable option for its supply quality and its carbon dioxide free energy cycle. Nevertheless, the traditional water based power conversion systems have reached technological limits and new ways are ought to be found. New heat transfer fluids have to be selected and qualified.

At the Institute of Neutron Physics and Reactor Technology (INR) of the Karlsruhe Institute of Technology (KIT), research in this area is taking place. Since 2012, the KASOLA facility, a Sodium Laboratory, is being built in order to investigate the development and qualification of computational fluid dynamics codes. This will allow developing and improving devices that use this technology.

1.2 Objectives of the project

The Karlsruhe Sodium Laboratory is a medium sized thermal-hydraulic test stand (around 700kW) and, thanks to its flexibility, it will allow to fulfil studies of heat transfer and storage and some more which will be discussed later on. Today, the construction of the facility is finished, and Set into Operation Experiments are being developed in order to test and qualify the facility. Before they are performed in the laboratory they will first be simulated with an specific software, using the TRACE code, which is a reactor system analysis code designed to analyse reactor transients and accidents up to the point of significant fuel rod damage.

The main objective of this project is, throughout the simulation of these test experiments, to analyse the facility in order to assure its reliability and performance.

Moreover, different situations for loss of coolant accidents will be studied, in order to know from the simulations the evolution over the time while these events occur and important aspects as the available reaction time or the magnitude of the damage. This will allow the development of better prevention and safety measures, as well as the preparation of the team to face such kind of problems.

At the end of the project, results will be analysed by the KASOLA team, who will take the presented information into consideration for the development of the research.

2 SODIUM IN POWER CONVERSION SYSTEMS

2.1 Material properties of sodium

Among other light metals, sodium has shown to have better properties for its use in power conversion system. The properties of sodium up to its melting point are good and very uniform, hence taken as constant. The following table contains some of the properties of sodium which need to be considered and also other materials have been included to show the advantages over them.

Properties (at $1,01 \cdot 10^5$ Pa)	Na	Pb	44,5% Pb 55,5% Bi	97,7% Pb 2,3% Mg	25% Na 75% K
Melting temperature (K)	370,85	600,55	396,55	521,85	262,15
Boiling temperature (K)	1156,15	2018,15	1943,15	1883,15	1057,15
Density at 773,15 K (kg/m^3)	883	10470	10050	9560	752
Thermal conductivity At 773,15 K (W/mK)	66	15,4	14,4	22	26,2
Specific heat capacity At 773,15 K (J/kgK)	1254	147	146	168	872
Kinematic viscosity At 773,15 K (m^2/s)	$29,0 \cdot 10^{-8}$	$17,6 \cdot 10^{-8}$	$12,8 \cdot 10^{-8}$	$15,3 \cdot 10^{-8}$	$23,4 \cdot 10^{-8}$

Table 2.1. Properties of sodium and other light metals in simulation conditions

2.2 Sodium-cooled fast reactors

Liquid sodium may be used as a coolant in a nuclear power plant. In general, light liquid metals allow a high power conversion density at low pressures. Besides this advantage, also corrosion, typical in the pipes of the heat exchanger of light water reactors, is avoided. On the other hand, sealing is an aspect of great concern, as sodium reacts strongly with water and air.

The working temperature of the sodium is around 500°C , below its boiling point. The cooling system of the reactor works at low pressures and high temperatures. The closed fuel cycle makes the regeneration of fissile fuel (plutonium and

uranium-mixed oxide) possible, since they operate with high energy neutrons making the fission of actinides more effective. It achieves a high level of safety though passive means. This kind of reactors have accumulated experiences over more than 400 years.

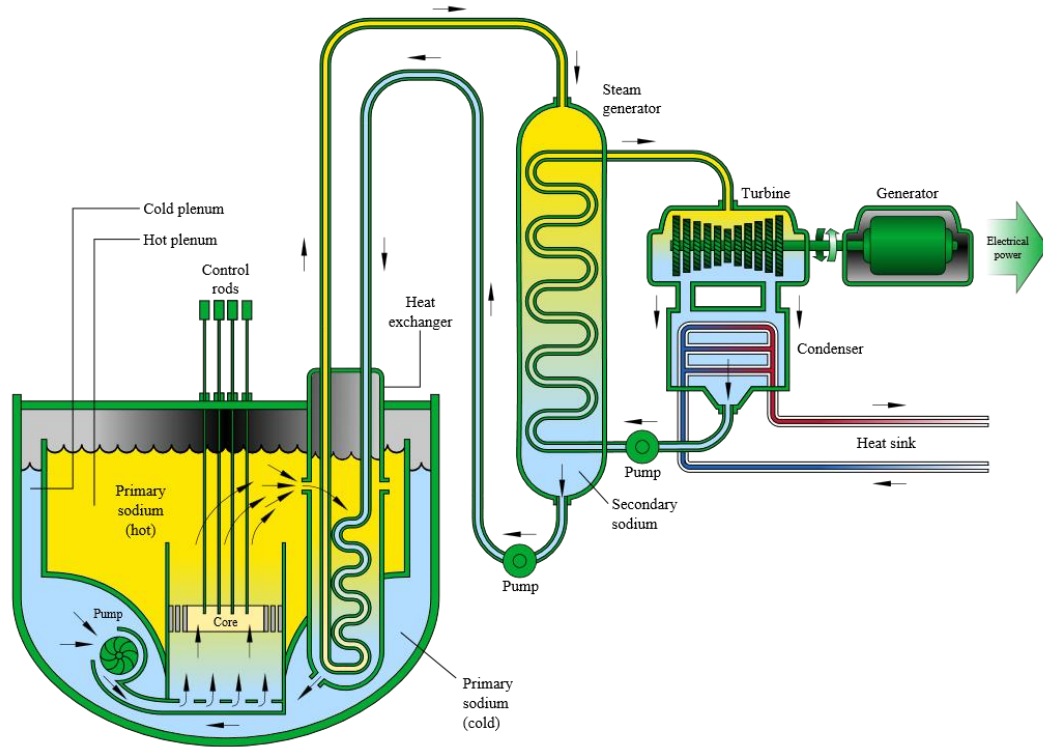


Figure 2.1. Principle of a pool-type sodium-cooled fast reactor.(A Technology Roadmap for Generation IV Nuclear Energy Systems)

In a Sodium-cooled fast reactor, in the primary system, sodium enters at a temperature of around 400°C at the bottom of the reactor and then heated up to $\sim 550^{\circ}\text{C}$. The primary system exchanges heat to a secondary sodium system, where the temperature is risen from around 350°C up to 500°C approx. This secondary system, will exchange heat with a steam generator, producing superheated steam at around 500°C and 12MPa that is sent to the steam turbine. As sodium is very reactive in contact with oxygen, it is protected at the reactor vessel with the inert gas Argon (Yoshiaki Oka, 2008).

2.3 Sodium in solar thermal power plants

On the other hand, its application as thermal storage medium in solar thermal power plants seems also promising. The reason is similar to the one in sodium-cooled fast reactors. Systems based on the Rankine cycle are limited in temperature and pressure. This is interesting for tower concentrating systems, as the liquid metals have the advantage of having heat transfer coefficients ten times higher as the molten salts, as well as lower melting points. This would mean a high cost reduction and a big efficiency increase. Also, innovative power conversion systems with sodium are already under study. One of them are the AMTEC-cells (Alkali metal thermal to electric converter), which show to have high efficiencies and no moving parts and produce direct current. (Application of liquid metals for solar energy systems, 2012)

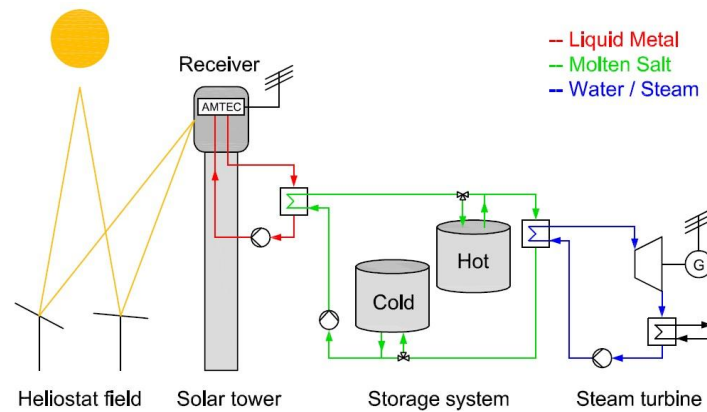


Figure 2.2. Scheme of an innovative sodium based conversion system with a secondary molten salt storage system (Conceptual study of central receiver systems with liquid metals)

3 KARLSRUHE SODIUM LABORATORY

3.1 Helmholtz Alliance LIMTECH

The investigation taking place in the KASOLA facility takes part in the Helmholtz Alliance on liquid metal technology (LIMTECH) and the Helmholtz Energy Materials Characterization Platform (HEMCP). LIMTECH covers the R&D activities on liquid metals as heat carriers including heat changes. The HEMCP was created to respond to the needs of more sophisticated energy systems, in order to be able to reach higher temperatures for better reactor efficiencies. The Karlsruhe Institute of Technology (KIT) is an important research centre and makes a significant contribution to the investigation in the energy field (besides other). The program-oriented research from the university is organized by the Helmholtz Association, created as an official representation of existing relationships between some independent research centres. Its main goal is to solve nowadays scientific challenges. The scientists belonging to this society participate in concerted national research programmes. Moreover, in the energy field, scientists work to develop solutions for an economically, ecologically and socially sustainable energy supply. Research is also done in nuclear fusion as a new sustainable energy source.

3.2 KASOLA overview

The KASOLA is a medium-sized (700 kW approx.) versatile experimental facility created to investigate flow phenomena in liquid sodium for nuclear and non-nuclear applications. The capacity of the whole facility is 7 m³ of sodium, moved by a magneto-hydrodynamic pump, and can be operated in a temperature range from 150-550°C. Its working flexibility allows a wide range of thermal-hydraulic experiments. At present, the purpose is to demonstrate that sodium is a feasible fluid for thermal storage system and direct energy conversion at high temperatures due to its low density and high thermal conductivity.

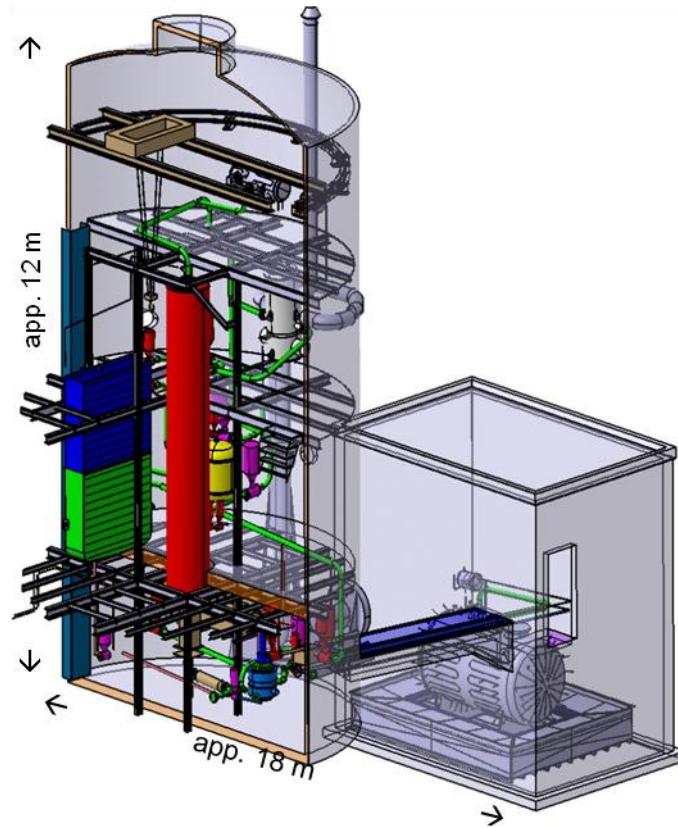


Figure 3.1. Section of a 3D model of the KASOLA facility

For the long term, it is expected to be capable of fulfilling the following tasks, among others:

- Validation and improvement of turbulent liquid metal heat transfer models in CFD tools on limited geometric scale.
- Flow pattern evaluation in rectangular channels and backward-facing step in heat transfer systems.
- Investigation of transition flow patterns from forced to free convection modes.
- Thermal-hydraulic investigation of flow patterns in fuel bundles or pool configurations in prototypes or scaled models.

3.3 Design

The facility is placed inside a cylindrical steel structure of 12.5 m height and a diameter of 7.7 m. The concept of KASOLA was finished in 2010 with a basic design, which had to be revised several times after the Fukushima accident in 2011. The test section was improved, making it more versatile, allowing the investigation of sodium as a heat transfer fluid for energy systems. The design of KASOLA was optimized to avoid risks of sodium leakages, its contact with water and sodium fires.

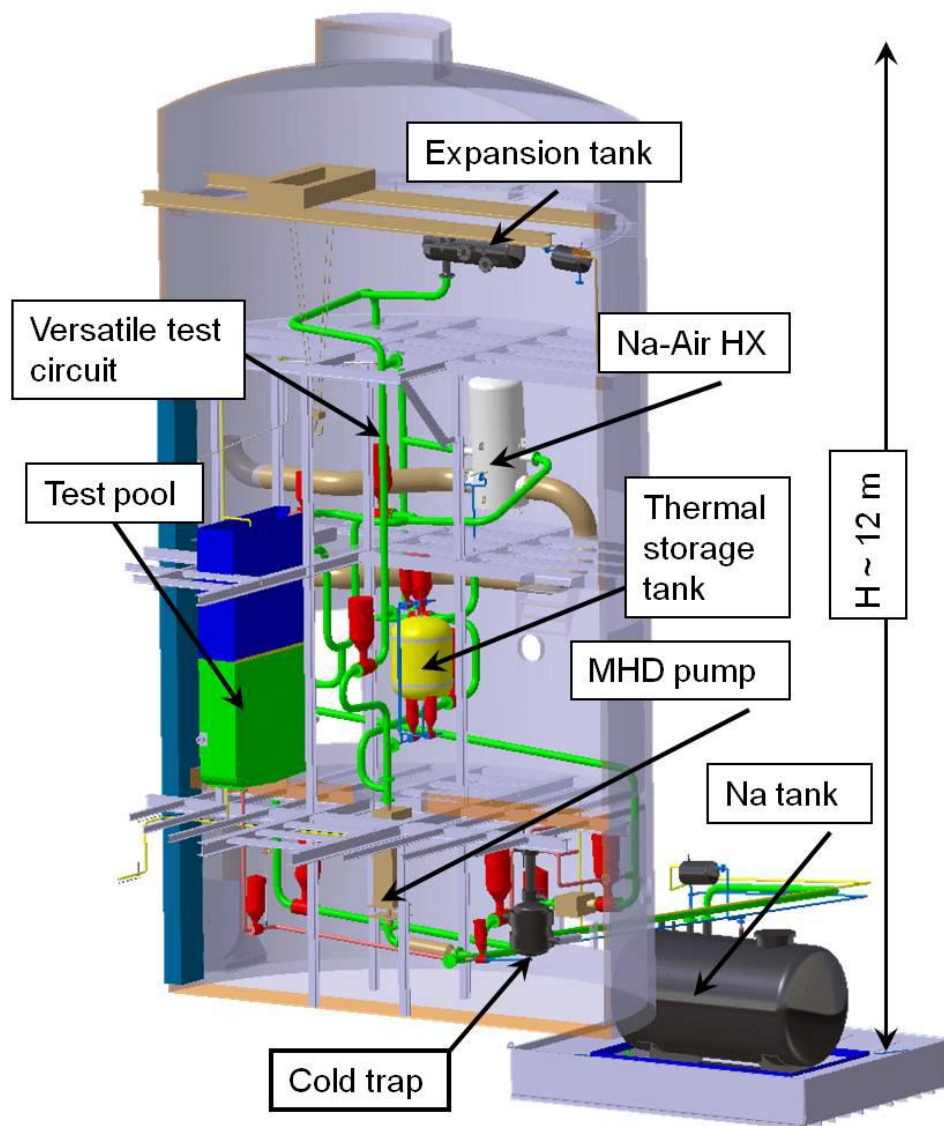


Figure 3.2. KASOLA loop inside the containment facility and the underground sodium storage.

The sodium system of KASOLA is divided in three subsections:

- Base loop with the cleaning section.
- Two test ports for experiments.
- Storage tank in a separate building apart from the cylindrical containment.

3.4 Base Loop

The base loop is the main part of the KASOLA facility. It is integrated by pipes, valves, a MHD pump, an air-sodium exchanger, expansion tank, cold trap, the cleaning and calibration section, the experimental ports, and the instrumentation and control.

Piping:

In the KASOLA facility, horizontal pipes are inclined by 4° to avoid sodium remnants when the loop is drained.

MHD pump:

The magneto-hydrodynamic pump is an induction pump used in KASOLA. Two different types may be used: a flat linear pump (FLIP) and a cylindrical pump (ALIP). This last one is integrated in the facility. Its performance has been increased by redesigning it, providing a flow rate of around $150\text{m}^3/\text{h}$ and a pressure head of 0.4MPa .

Magnetic mass flow meter:

It is used to accurately calculate the average velocity of the fluid, in order to obtain the hydraulic and magnetic Reynolds number. It is done by measuring the voltage induced by the flow.

Coriolis mass flow meter:

Used as a reference measuring system for the magnetic flow meter, since its capabilities may decay with the time. This allows its accurate calibration, always up to a temperature of 210°C .

Heat exchanger:

In the sodium-air heat exchanger sodium is cooled down. It consists of a U-tube HX and it is designed to dissipate 400kW to the cold air. The air cooling circuit is composed by a ventilator, a heater that warms up the HX tubes before it is filled up with sodium and valves that control the cooling capacity. The valves isolate the air section from the environment in the facility, in case a sodium leakage occurs.

Expansion tank:

The expansion tank ensures a safe operation as it absorbs the volume difference when the working temperature is higher or lower. It is placed in the highest point of the circuit and has a volume of 0.3m³. The upper, middle and lower levels are monitored by means of four electrodes.

Sodium separator:

The sodium separators are placed behind the storage tank and the expansion tank to prevent the contamination of the cover gas system with sodium aerosol droplets. These droplets freeze on the internal surfaces of the separator.

Thermal insulation:

Maximal temperature can be reached in the hot-leg (550°C); here the thermal insulation has a thickness of 200mm. As the rest of the loop is at lower temperature, the insulation is thinner, varying between 100 and 150 mm.

3.5 Support and safety system

Cleaning loop:

It comprises the magneto-hydraulic pumps, the magnetic flow meter and the cold trap. It allows a fast release of the sodium into the storage tank.

Storage tank:

It is designed to store the liquid sodium when the facility is not being used or under maintenance. Argon at a subatmospheric pressure between 0.12-0.14 MPa

prevents the sodium to have contact with air. It has a capacity of 8 m³ and supports a pressure of 0.52 MPa at 450°C.

3.6 Capabilities

As it has been already remarked, the KASOLA facility may be defined by its flexibility as it allows a large spectrum of tests. The basic loop has a versatile test section which permits different flow configurations. Multiple test ports are foreseen for different experiments. There are several test ports designed for different experiments.

Pool simulator:

This test port was designed for a scale simulation of the primary system of a pool reactor. In the KASOLA base loop, the heat sink would take place, simulating the secondary system.

Versatile test section:

KASOLA's test section has a 6m height, separating the expansion tank from the pump's outlet, and several experiments can be performed.

- Natural convection can be studied, when a local cooler section on the pump's outlet pipe is installed and a section is heated, while it is working with the heat exchanger.
- For the study of sodium as a heat transfer and storage fluid in new concentrating solar power systems and nuclear power plants.
- Backward facing step (LIMTECH A1):

In this experiment, the influence of a BFS on the temperature distribution of sodium is investigated. It will allow the study vortices and flow perturbations for code development.

- Transition between free, mixed and forced convection (LIMTECH B1):

This investigation looks forward to a smooth transition from forced convection to free convection, for an optimal design.

4 NUMERICAL SIMULATION SOFTWARE

For the realization of this project, the specialized numerical simulation code TRACE will be used. The Symbolic Nuclear Analysis Package (SNAP) graphic interface will serve to easily handle TRACE. The AptPlot software, a plotting tool, is used to analyse and monitor the results of the calculations.

4.1 The TRACE code

While the technology of nuclear power plants developed, getting more sophisticated, reactor systems codes have become of great use. Thermo-hydraulic simulation allows the study of transient cases which theoretical models or human reasoning are not capable to solve.

Since the last century, the U.S. Nuclear Regulatory Commission (USNRC) has worked in the development of advanced codes for analysing the neutronic-thermal-hydraulic behaviour in nuclear reactors during real and hypothetical scenarios. The validation of these codes is done by carrying out experiments at small scales, and the results are used to implement improvements in such codes. This helps to take decisions concerning the plant design, operation and safety.

TRAC/RELAP Advanced Computational Engine (TRACE) is a modern lumped parameter code, designed to analyse break loss of coolant accidents (LOCA) and system transients.

In an accident of the type LOCA, one of the pipes of the primary circuit has a break in it. The cooling fluid is discharged into the environment and, in the case of sodium; this can have severe consequences as it is highly reactive on contact with air or water.

TRACE main physical models

TRACE fluid field equations

For the modelling of two-phase flows, TRACE uses the averaged Navier-Stokes equations in each phase. They consist of separate mass, energy and momentum

conservation for the liquid $[X_l]$ and gas $[X_g]$ fields, leading to six separate partial differential equations:

- Mass conservation equations

$$\frac{\partial}{\partial t}[(1 - \alpha)\bar{\rho}_l] + \nabla \cdot [(1 - \alpha)\bar{\rho}_l \vec{u}_l] = -\bar{\Gamma}$$

$$\frac{\partial}{\partial t}(\alpha\bar{\rho}_g) + \nabla \cdot (\alpha\bar{\rho}_g \vec{u}_g) = \bar{\Gamma}$$

Where $\Gamma = \frac{h_l \cdot A_w \cdot (T_w - T_l)}{V \cdot (h_g - h_l)} + \frac{q_{il} + q_{ig}}{h_g - h_l}$

- Momentum conservation equations

$$\frac{\partial}{\partial t} \vec{u}_l + \vec{u}_l \cdot \nabla \vec{u}_l = -\frac{1}{\rho_l} \nabla P + \frac{f_i - \Gamma(\vec{u}_l - \vec{u}_l) + f_{wl}}{(1 - \alpha)\rho_l} + \vec{g}$$

$$\frac{\partial}{\partial t} \vec{u}_g + \vec{u}_g \cdot \nabla \vec{u}_g = -\frac{1}{\rho_g} \nabla P + \frac{f_{wg} - f_i - \Gamma(\vec{u}_g - \vec{u}_l)}{\alpha\rho_g} + \vec{g}$$

- Energy conservation equations

$$\begin{aligned} \frac{\partial}{\partial t}[(1 - \alpha)\rho_l e_l + \alpha\rho_g e_g] + \nabla \cdot [(1 - \alpha)\rho_l e_l \vec{u}_l + \alpha\rho_g e_g \vec{u}_g] \\ = -P \nabla \cdot [(1 - \alpha)\vec{u}_l + \alpha\vec{u}_g] + q_{wl} + q_{wg} + q_{dl} + q_{dg} \end{aligned}$$

$$\begin{aligned} \frac{\partial}{\partial t}(\alpha\rho_g e_g) + \nabla \cdot (\alpha\rho_g e_g \vec{u}_g) \\ = -P \frac{\partial}{\partial t} \alpha - P \nabla \cdot (\alpha\vec{u}_g) + q_{wg} + q_{dg} + q_{ig} + \Gamma h_v' \end{aligned}$$

(TRACE V5.0 Theory Manual)

TRACE description

TRACE is, as said, an advanced and precise computational code for the study of the thermo-hydraulic behaviour of light water nuclear reactors. It is designed to perform best-estimate analyses of different accident scenarios. Is a code for finite-volume, two-phase compressible flows and can model heat structures and control systems that interact with component models and the fluid solution.

With the code, each component can be divided in some number of cells, where the equations of mass, momentum and energy conservation are solved. For TRACE to solve the calculation a model (dimensions and geometry) must be defined. Heat structures and control systems can also be integrated.

In order to manage with the code, the SNAP graphic interface is used, of which the greatest advantage is the ability to create a model simply by adding components like pumps, valves or control blocks and to easily change their properties. Its flexibility highly allows the creation and edition of the input as well as monitoring of results and interaction with the code. The AptPlot tool can read the TRACE code resulting from a simulation, and can represent in 2D the output of any component of the model. This software can be either managed in Microsoft Windows or in Linux (Symbolic Nuclear Analysis Package (SNAP) User's Manual).

5 DESCRIPTION OF THE KASOLA TRACE MODEL

For the simulation of the KASOLA facility, an approach has been done with the TRACE code. The components of the whole system were modelled and joined as the figure shows. Afterwards, for this thesis, some additions have been done.

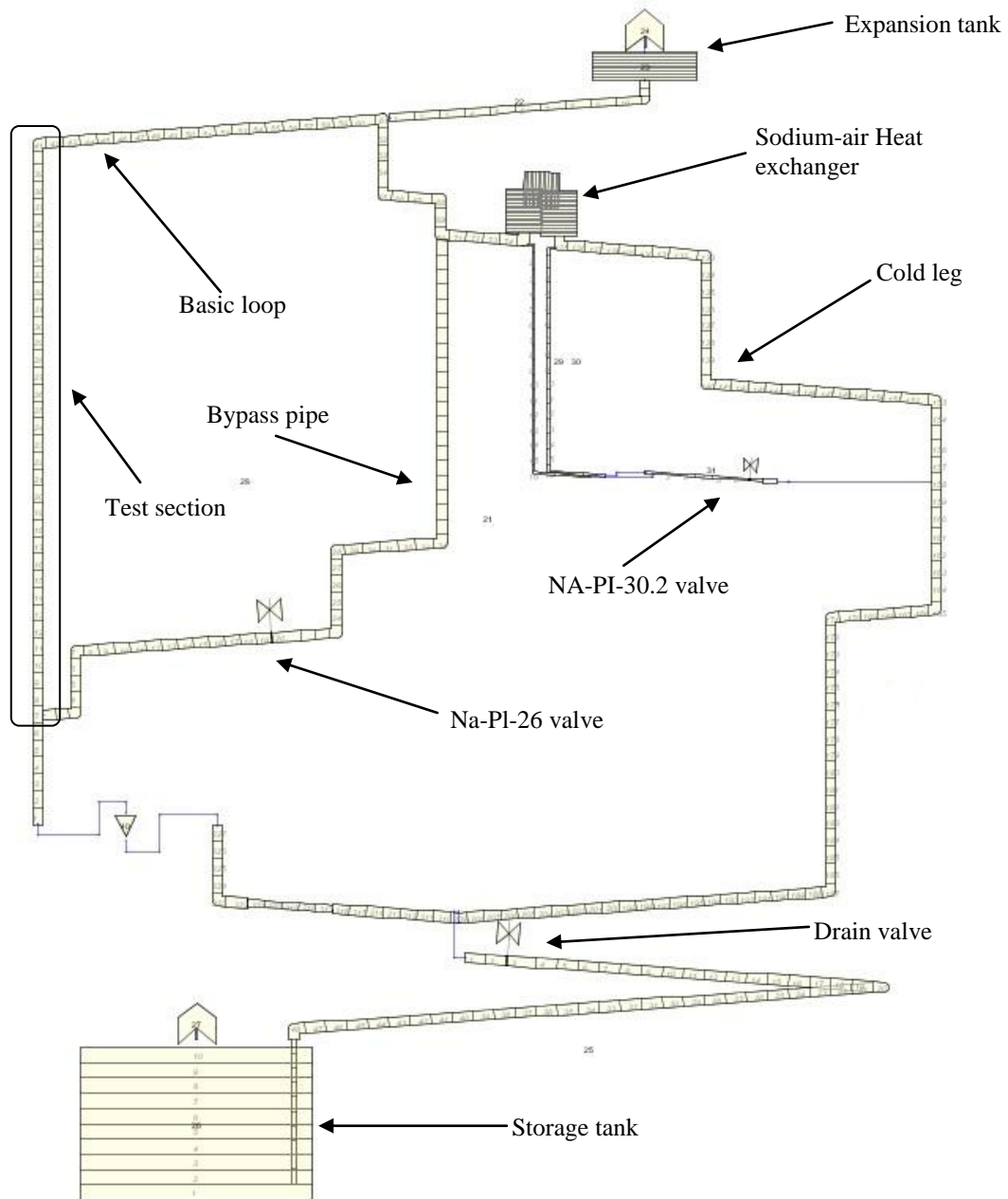


Figure 5.1 Detail of the KASOLA model and the hydraulic components

Among the main systems, the Basic Loop can be found, which is the main and largest component of the model. It contains all the piping and the heat exchanger. The valves have been modelled as a separate component.

5.1 TRACE components for KASOLA

TRACE User's guide has integrated a complete description of the available components to be used. The following elements were used in the extension of the KASOLA model:

- **BREAK**

The BREAK is the outflow component of the system and consists on a single hydrodynamic cell used to model the fluid properties, the desired coolant-flow and the pressure boundary conditions at the end of any 1D hydraulic component (like PIPE). For LOCA simulation, a BREAK shall be used for the representation of the outflow of the cooling fluid.

- **PIPE**

It is used to model the fluid flow in a 1D pipe for the connection between components of a system. The boundary conditions are defined by a BREAK and/or a FILL component. It can be divided in a limited number of fluid cells. Moreover, the geometry of each cell can be specified in the properties of the component. In each cell, conservation of mass, momentum and energy equations are solved. It also allows adding heat structures to the pipe walls.

- **SINGLE JUNCTION**

The PIPE component is treated as single junction when it has no cells (no volume).

- **VALVE**

The VALVE component has similar features to those of the PIPE component. It is used to model the flow through a 1D pipe with a variable flow area. Variable control is done over one internal cell face, where the

valve is placed. This flow area can be fixed or be set to change at a constant rate.

- **Control Block**

Control blocks are mathematical functions that operate on zero or more input variables, giving an output signal. This output signal can be the input variable for another control block but also any signal variable.

- **Signal Variable**

Signal variables define the input variables for control blocks and trip signals. They provide the information from the thermal-hydraulic model to the control system.

(TRACE V5.762 User's Guide Volume 2: Modeling Guidelines)

5.2 Hydraulic components

For every component, the geometry and the boundary and initial conditions have to be set. The main fluid dynamic parameters have to be set for every component.

- **Basic loop:** *Pipe 21.*
- **Expansion tank:** *Pipe 23.*
- **Storage tank:** *Pipe 26.*
- **Drain:** *Valve 25.*
- **Na-Pl-26:** *Valve 28.*
- **Na-Pl-30.2:** *Valve 31.*
- **Break 1:** *Valve 10, Break 20.*
- **Break of the instrumentation pipe:** *Pipe 60, Valve 50 and Break 70.*
- **Break into the insulation:** *Valve 50, Pipe 60, Pipe 20 and Break 10.*

Name	Component Type	Number of cells	Length/ volume	Hydraulic diameter	Initial pressure	Initial temperature
Basic loop	Pipe	227	~37 m	$105,3 \cdot 10^{-3}$ m	$1,5 \cdot 10^5$ Pa	415,15 K
Expansion tank	Pipe, Break	10	0,3 m ³	-	$1,5 \cdot 10^5$ Pa	415,15 K
Storage tank	Pipe, Break	10	8 m ³	-	$1,5 \cdot 10^5$ Pa	415,15 K
Drain line	Valve	58	(*)	$105,3 \cdot 10^{-3}$ m	$1,5 \cdot 10^5$ Pa	415,15 K
Bypass line Na-PI-26	Valve	54	(*)	$105,3 \cdot 10^{-3}$ m	$1,5 \cdot 10^5$ Pa	415,15 K
HX Drain Na-PI-30.2	Valve	8	(*)	$16 \cdot 10^{-3}$ m	$1,5 \cdot 10^5$ Pa	415,15 K
Break 1	Valve, Break	2	~0 m	$8,8 \cdot 10^{-3}$ m	$1,5 \cdot 10^5$ Pa	415,15 K
Break of the instrumentation pipe	Pipe, Valve, Break	10	0,25 m	$8,8 \cdot 10^{-3}$ m	$1,5 \cdot 10^5$ Pa	415,15 K
Break into the insulation	Pipe, Valve, Break	40	2 m	$27,1 \cdot 10^{-3}$ m	$1,5 \cdot 10^5$ Pa	415,15 K

Table 5.1. Geometrical and initial values at each cell for every component. (*) The length of the basic loop encloses the drain line, bypass line and HX drain.

5.3 Control Blocks

- **Problem time:** TIMEOF 1



Figure 5.2. Time control block in SNAP interface

6 SIMULATION AND RESULTS

Each scenario will be analysed in detail below, including the description, modifications to the original model, properties and results. In each case, the temporal behaviour of the facility will be discussed, determining the total sodium loss through the breaks. An explanatory table is below shown, with an overview of the main features of the simulated scenarios.

Scenario	Break size	Drainage valve opening	Opening time	HX and Bypass valves opening
Drainage				
Drain 1	DN 8	No	20 seconds	No
Drain 2		No	20 seconds	Yes
Drain 3		Yes	20 seconds	No
Drain 3 (M)		Yes	60 seconds	No
Drain 4		Yes	20 seconds	Yes
Drain 4 (M)		Yes	60 seconds	Yes
Instrumentation Pipe				
Instr. 1	DN 8	No	20 seconds	No
Instr. 2		No	20 seconds	Yes
Instr. 3		Yes	20 seconds	No
Instr. 3 (M)		Yes	60 seconds	No
Instr. 4		Yes	20 seconds	Yes
Instr. 4 (M)		Yes	60 seconds	Yes
Break and flow through the insulation				
Porous 1	DN 25	No	20 seconds	No
Porous 2		No	20 seconds	Yes
Porous 3		Yes	20 seconds	No
Porous 3 (M)		Yes	60 seconds	No
Porous 4		Yes	20 seconds	Yes
Porous 4 (M)		Yes	60 seconds	Yes

Table 6.1 Overview of the features of each scenario

6.1 Steady-State simulation

Before the start of any transient simulation, it is necessary to prove the stability of the model. This is selected in the *Model Options* section in SNAP. In order to do it, the limit calculation time is set to 400 seconds, enough to reach the steady state. The convergence criterion for the steady-state calculation is set to 1.0E-04, the value suggested by the software. After running the simulation, the steady-state

conditions are reached after 135,1 seconds. Taking this information into account, it will be set that the transient state starts after the first 140 seconds of the simulation. The temperature is constant at 415,15 K and the pressure, with an initial value of $1,5 \cdot 10^5 \text{ Pa}$, when steady state is reached, increases up to $2,2 \cdot 10^5 \text{ Pa}$.

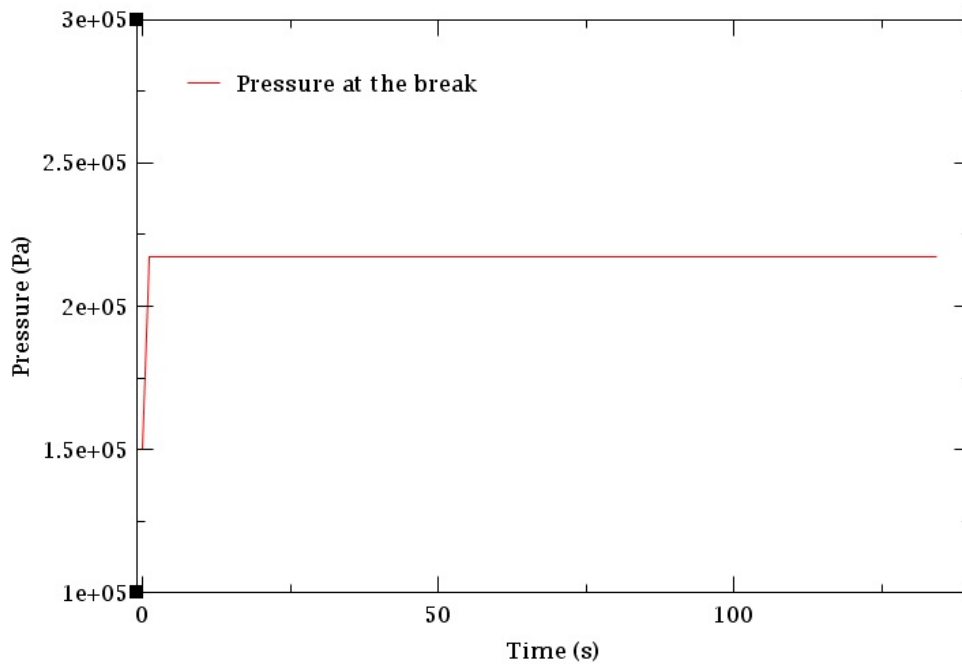


Figure 6.1. Pressure convergence at the steady state simulation

6.2 Drainage simulation for small break at the basic loop

6.2.1 Transient scenario definition

Beyond the original model, three different drainage cases are going to be simulated. This scenario represents the possible break of an instrumentation pipe inside the insulation, as if it was a welding failure. LOCA will be simulated in all of them, a one or several breaks into the environment with a pressure of 1,01bar and isothermal conditions. The first one will have one break; the second, two and, the third, three. Each of the cases will contain several valve configurations, including an approach to what a manual opening of the drain valve would be. This will allow analysing a more extreme situation, allowing to see how much sodium would be lost in the worst case.

In this section the results of the simulation from the small break of an instrumentation pipe at its welding point with the basic loop are exposed. Six different simulations have been carried out. In each of them a different configuration of the valves from KASOLA is proposed, as it is below explained, and they are classified in the following way:

Scenario	Valve opening configuration					
	NA-VSR-01		NA-VSR-06		NA-VI-02	
	Initial	Final	Initial	Final	Initial	Final
Drainage 1	0 %	0 %	0 %	0 %	0 %	0 %
Drainage 2	0 %	0 %	100 %	100 %	100 %	100 %
Drainage 3	0 %	100 %	0 %	0 %	0 %	0 %
Drainage 3 (M)	0 %	100 %	0 %	0 %	0 %	0 %
Drainage 4	0 %	100 %	100 %	100 %	100 %	100 %
Drainage 4 (M)	0 %	100 %	100 %	100 %	100 %	100 %

Table 6.2. Valve configuration for each scenario

6.2.2 Modifications over the original KASOLA model

In each case, the break is located on the cold leg at a height of 2,65m above the drain valve. It consists on a two cell valve (*Valve 10*) which connects the basic loop with a break (*Break 20*), as shown in the figure:

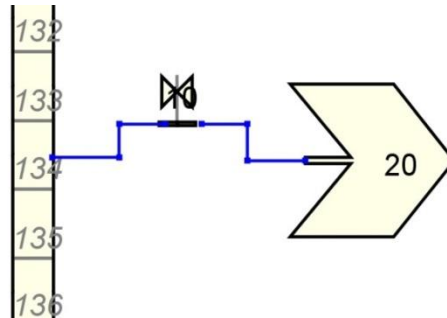


Figure 6.1: Break geometry

The size of the break is said to be the same as a DN 8 pipe (8.8 mm), introduced in the properties of the valve as the hydraulic diameter. A table with the initial values, included in the model, is shown below:

	Facility	Atmosphere
Pressure	$1.5 \cdot 10^5 \text{ Pa}$	$1.01 \cdot 10^5 \text{ Pa}$
Gas volume fraction	0.0	1.0

Table 6.3 Initial Conditions of the facility

The valve is maintained closed for the first 140 seconds and it is opened within 2 seconds, letting the sodium flow out of the facility.

- Drainage 1

The scenario presents a sodium leakage into the containment of KASOLA, where the valves from the cold leg (*NA-VSR-06/Valve 31*) and the hot leg (*NA-VI-02/Valve 28*) are closed, as well as the drain valve (*NA-VSR-01/Valve 25*). As it is seen, the process takes a considerable amount of time. This happens because the sodium will only flow through the break, until they are at the same height.

- Drainage 2

In this scenario, the drain valve is blocked, but the other two, the hot leg and the cold leg valves are left opened during the whole simulation. As well as in the Drainage 21, the simulation is made to be running for a larger amount of time.

- Drainage 3

As soon as the break appears, the drainage valve is opened. This allows the possibility to save a greater amount of sodium. A delay of 20 seconds in the opening time of the valve has been set, in order to consider the reaction time for the operator actions. The valves from the hot and cold leg are left closed. A manual opening of the drainage valve is also simulated, taking a reaction time of 20 seconds and an opening time of 60 seconds.

- Drainage 4:

In this scenario, drain valve is also opened as soon as the break happens, and a delay of 20 seconds has also been taken into account. The other two valves, are left opened during the whole simulation. In this case, also a manual opening of the drainage valve is taken into account.

6.2.3 Modifications over the heat exchanger

A small remark is that after the first simulations were done, some peaks in the mass flow rate graph were found. These peaks corresponded to the emptying of

the heat exchanger. It has been seen that the cells of the HX have a volume 14 times bigger than the cells of the basic loop. In order to have a more precise solution, the cells have been renodalized, splitting them into 7 uniform cells, as it is below shown.

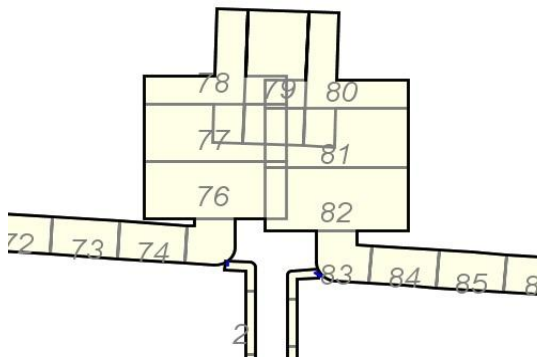


Figure 6.3. Heat exchanger before renodalization

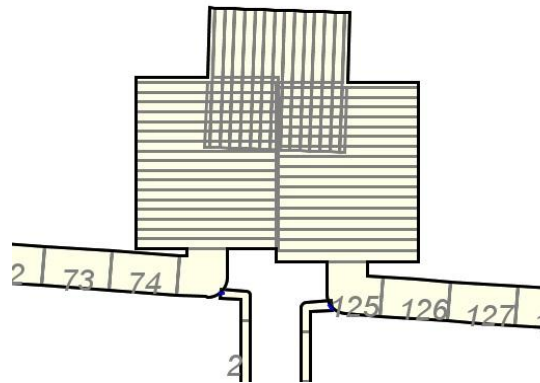


Figure 6.4. Heat exchanger after renodalization

This modification, has improved the simulation time, as well as the curve of the graph.

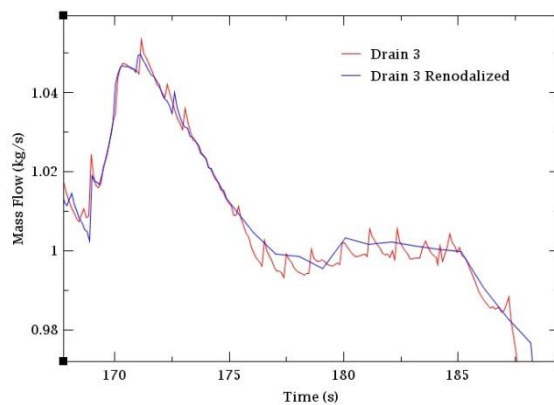


Figure 6.5. Detail of the mass flow rate of the HX in Drain 3 after the renodalization

Since the heat exchanger is a spot where the air and the sodium interact, it is important to have a good representation of the component, being critical a break at this location. A failure inside it can provoke a fire while there is sodium in it and it could not be stopped until it empties. Therefore it is meaningful the knowledge of the maximal time the heat exchanger would take to discharge. From the studied

cases, except for the third one, when the drainage valve is closed, the heat exchanger takes around 300 seconds to get empty and around 10 seconds when it is opened. During this time, at least, the sodium would react with the air.

6.2.4 Simulation of the transient and results

The results for the six scenarios are shown below. They are placed together in each graph to allow comparison between them through the simulation time.

For calculating the simulation, in the model options section from SNAP, the general conditions of the computation have to be set. The cooling fluid is selected as sodium, the type of analysis (transient or steady state) and the time step data have to be specified. The timestep will be reduced as soon as the break appears, in order to get a more accurate result. A problem end time of 2000 seconds is specified when the drain valve is closed during the whole simulation.

End Time	Minimum Size	Maximum Size	Heat vs Fluid Size	Max Conv. Power Diff	Long Edit Interval	Graphics Interval	Restart Interval	Short Edit Interval
10.0	1.0E-9	0.1	10.0	1.0E20	10.0	1.0	10.0	10.0
130.0	1.0E-9	0.5	10.0	1.0E20	100.0	1.0	100.0	100.0
500.0	1.0E-9	0.1	10.0	1.0E20	100.0	0.1	100.0	100.0
2000.0	1.0E-9	0.1	10.0	1.0E20	100.0	1.0	100.0	100.0

Table 6.4. Timestep data table for scenarios 1 and 2

When the drain valve is opened after the break appears (Drainage 3 and 4), an end time of 400 seconds will be set, as the following table shows.

End Time	Minimum Size	Maximum Size	Heat vs Fluid Size Ratio	Max Conv. Power Diff	Long Edit Interval	Graphics Interval	Restart Interval	Short Edit Interval
10.0	1.0E-9	0.1	10.0	1.0E20	10.0	1.0	10.0	10.0
135.0	1.0E-9	0.1	10.0	1.0E20	100.0	1.0	100.0	100.0
175.0	1.0E-6	0.1	10.0	1.0E20	100.0	0.1	100.0	100.0
400.0	1.0E-6	0.1	10.0	1.0E20	100.0	1.0	100.0	100.0

Table 6.5: Timestep data table for scenarios 3 and 4

In cases 1 and 2, the simulation stops after 900 seconds approximately. In the cases 3 and 4 they take around 250 seconds to drain the whole sodium. The total mass loss and the mass flow rate through the break are shown.

The total lost mass is calculated and plotted using the integration tool of AptPlot.

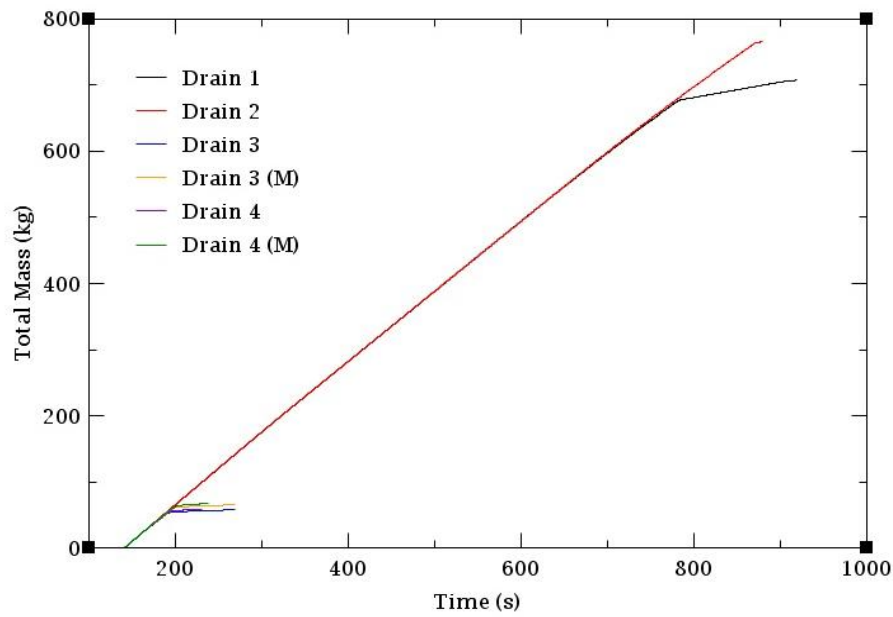


Figure 6.6. Drainage Accumulated mass loss

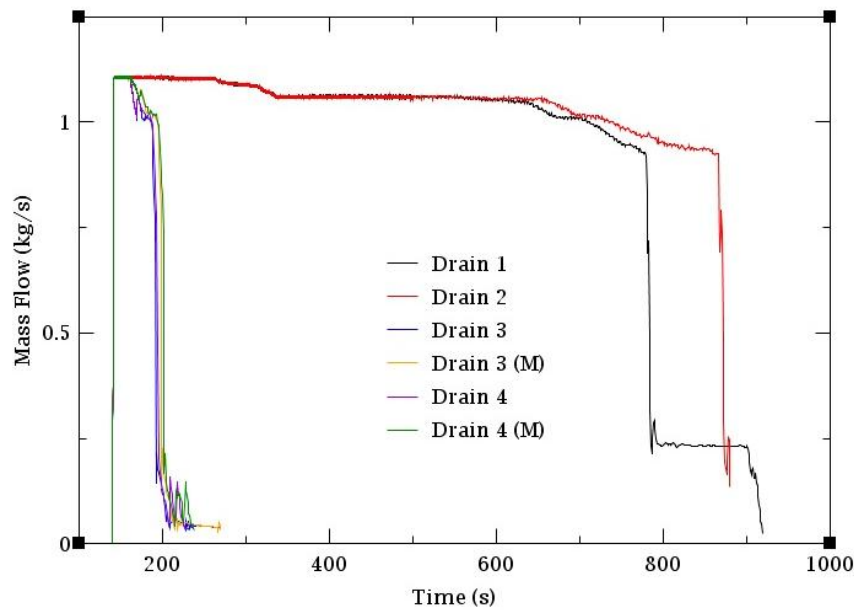


Figure 6.7. Drainage Mass flow rate

Firstly, looking at the mass flow rates of cases 1 and 2, it can be seen that there are some changing points in the graph. After 140 seconds, break appears and sodium starts to flow through it. Mass flow is constant until 275 seconds have gone by. At this point, the expansion tank is empty and the basic loop starts to drain. This decrease stops after around 375s, where the heat exchanger starts its draining with a constant mass flow rate. This process finishes after 650th seconds.

Then, the rest of the basic loop drains at a progressively decreasing mass flow rate. In case 1, after 780 seconds, flow drops drastically and remains constant around 0.25 kg/s for approximately 100 seconds. This is due to the remaining sodium at the left hand side of the basic loop, making pressure until it is at the same level as the break. This happens because the valves at the hot and cold legs are closed. In the second case, these valves are open, and the sodium in the facility, decreases at the same level. Also, no sodium can be retained by these valves and, so, more amount of coolant is lost, as the plots show. It appears, that after the drastic drop in the mass flow rate of sodium, argon gas is started to be released into the environment, flowing through the break. This will be seen in the rest of experiments and happens because the pressure boundary condition is set in the model to $1,5 \cdot 10^5 \text{ Pa}$ and it is constant inside the facility. This means, that if the simulation runs for an infinite amount of time, it will be always releasing gas into the environment. This is an aspect to be improved in further projects.

As the cases 3 and 4 take much less time to be simulated than the first two, in order to appreciate them better, a graph is shown below.

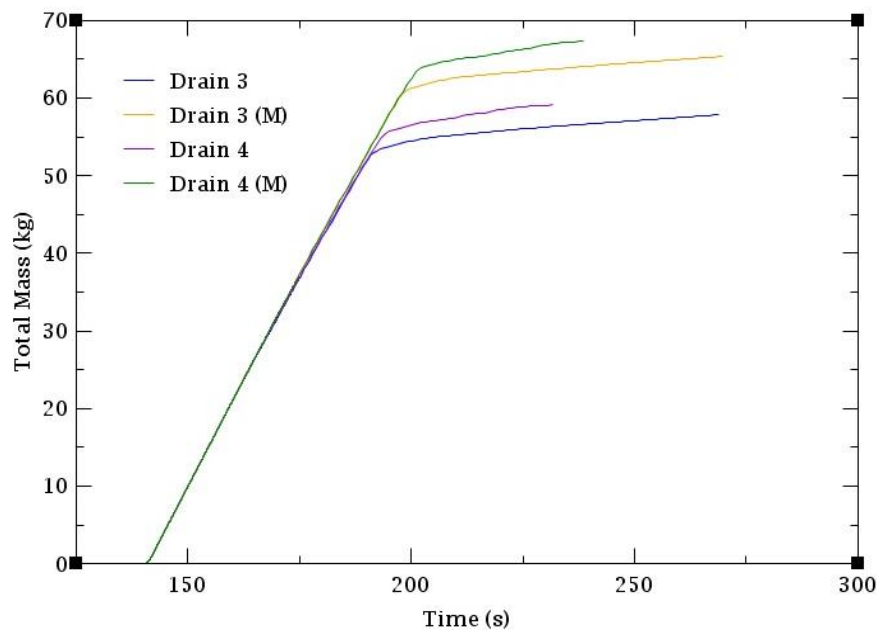


Figure 6.8. Drainage accumulated mass loss for cases 3 and 4

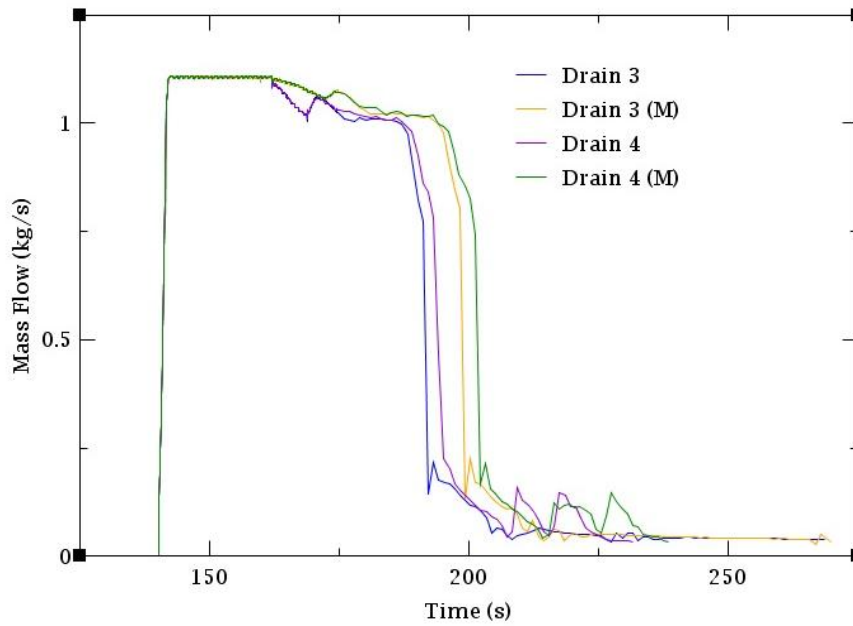


Figure 6.9. Drainage mass flow rate for cases 3 and 4

It can be seen that both cases and the simulations of the manual opening follow a similar pattern in the mass flow rate graph. As we know, the break appears after 140 seconds, and the mass flow rate remains constant until the drainage valve is opened. At this time, mass flow starts to decrease progressively, as the whole facility empties. From the second 175 to the 185, the heat exchanger empties, and the flow through the break is constant. After this point, there is a big drop in the mass flow rate, as the facility has been emptied, but does not decrease to zero as some sodium may still be dripping.

The total lost sodium mass is detailed in the table below, for each case, including also the last value for the mass flow rate.

Scenario	Problem time	Total mass loss	Mass flow rate residuals
Drain 1	919.000 s	707.271 kg	0.025 kg/s
Drain 2	880.238 s	765.772 kg	0.134 kg/s
Drain 3	231.612 s	57.841 kg	0.037 kg/s
Drain 3 (M)	238.603 s	65.352 kg	0.033 kg/s
Drain 4	231.609 s	59.128 kg	0.033 kg/s
Drain 4 (M)	238.63 s	67.331 kg	0.032 kg/s

Table 6.6. Drainage problem final values

As it can be seen, at the end of the simulation, the mass flow rate is really low. Opening the drainage valve manually means a mass loss of around 8 kg of

sodium, as if it was opened electrically. Also, having the cold and hot leg valves open would mean a loss of between 1 and 2 kg of sodium for cases 3 and 4 and almost 60 kg for cases 1 and 2.

6.3 Instrumentation pipe break simulation out of the insulation

6.3.1 Transient scenario definition

In this case, a more realistic scenario is analysed. The instrumentation pipes that go from the basic loop or component to the sensor, suffer a cross section change (from DN 8 to DN 6) when it is out of the insulation. This joining point may fail and provoke a break. In this case, sodium would be released into the environment of the KASOLA containment, bypassing the insulation. The cross section change is located around 100 mm away from the insulation, 250 mm away from the basic loop pipe. This will be modelled as a thin pipe connected to the basic loop. At the end of the pipe, a valve is placed, connecting it to a break. For each component, geometry, properties and initial values of the temperatures and pressures are given. As in the previous experiment, the break appears after running the simulation for 140 seconds, when the valve opens. The same valve configurations have been also used. The same valve configuration from the previous experiment will also be used in this one.

Scenario	Valve opening configuration					
	NA-VSR-01		NA-VSR-06		NA-VI-02	
	Initial	Final	Initial	Final	Initial	Final
Instrumentation Pipe 1	0 %	0 %	0 %	0 %	0 %	0 %
Instrumentation Pipe 2	0 %	0 %	100 %	100 %	100 %	100 %
Instrumentation Pipe 3	0 %	100 %	0 %	0 %	0 %	0 %
Instrumentation Pipe 3 (M)	0 %	100 %	0 %	0 %	0 %	0 %
Instrumentation Pipe 4	0 %	100 %	100 %	100 %	100 %	100 %
Instrumentation Pipe 4 (M)	0 %	100 %	100 %	100 %	100 %	100 %

Table 6.7. Valve configuration for each scenario

6.3.2 Variations over the original KASOLA model

In each scenario, the break is located in the same place as in the previous experiment (2,65m over the drain valve). It consists on a thin DN 8 horizontal

pipe (*Pipe 60*) connected to the basic loop, a dimensionless valve (*Valve 50*) which connects the pipe with a break (*Break 70*), as shown in the figure:

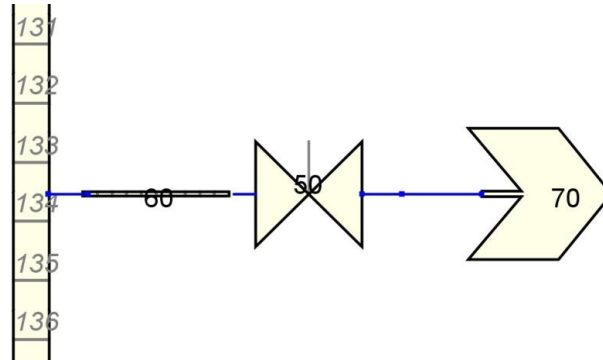


Figure 6.10. Instrumentation pipe geometry

The roughness of the pipe is the same as in the rest of the stainless steel components of KASOLA, like the basic loop, which is $\epsilon = 3.0 \cdot 10^{-5} \text{ m}$.

6.3.3 Simulation of the transient and results

Below, the results of the simulation are shown. The temporal behaviour of the facility when the break appears and its reaction to the activation of the fast drain will be analysed. Cases 1 and 2 are run for 2000 seconds, and the others for 400 seconds. Therefore, the timestep values are set to be the following, according to the said simulation times:

End Time	Minimum Size	Maximum Size	Heat vs Fluid Size Ratio	Max Conv. Power Diff	Long Edit Interval	Graphics Interval	Restart Interval	Short Edit Interval
90.0	1.0E-9	0.5	10.0	1.0E20	100.0	1.0	100.0	100.0
175.0	1.0E-9	0.1	10.0	1.0E20	100.0	0.1	100.0	100.0
400.0	1.0E-8	0.1	10.0	1.0E20	10.0	1.0	10.0	10.0
2000.0	1.0E-9	0.1	10.0	1.0E20	100.0	1.0	100.0	100.0

Table 6.8. Timestep data table for scenarios 1 and 2

End Time	Minimum Size	Maximum Size	Heat vs Fluid Size Ratio	Max Conv. Power Diff	Long Edit Interval	Graphics Interval	Restart Interval	Short Edit Interval
10.0	1.0E-9	0.1	10.0	1.0E20	10.0	1.0	10.0	10.0
135.0	1.0E-9	0.1	10.0	1.0E20	100.0	1.0	100.0	100.0
175.0	1.0E-6	0.1	10.0	1.0E20	100.0	0.1	100.0	100.0
400.0	1.0E-6	0.1	10.0	1.0E20	100.0	1.0	100.0	100.0

Table 6.9. Timestep data table for scenarios 3 and 4

Below, the mass flow rate out of the loop and the total lost mass is shown.

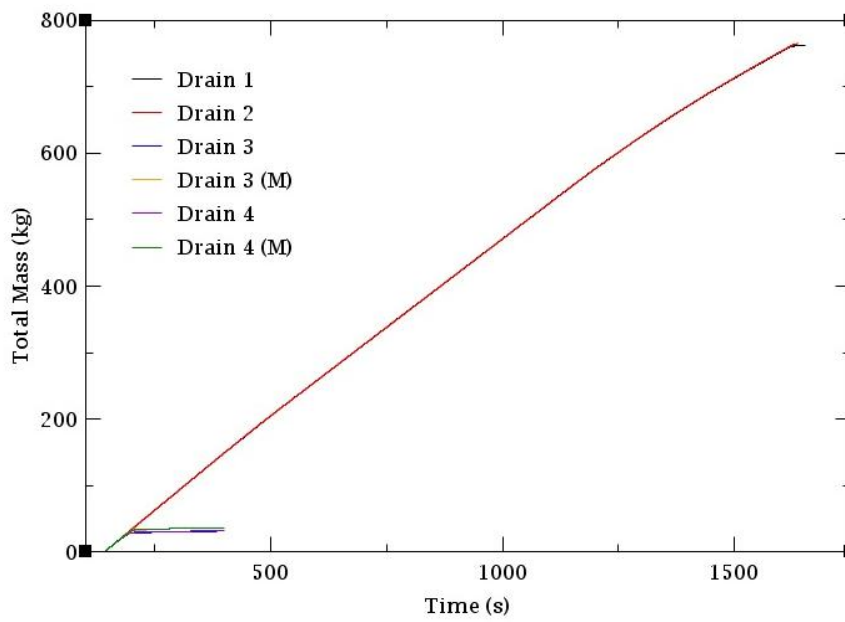


Figure 6.11. Instrumentation Pipe Accumulated mass loss

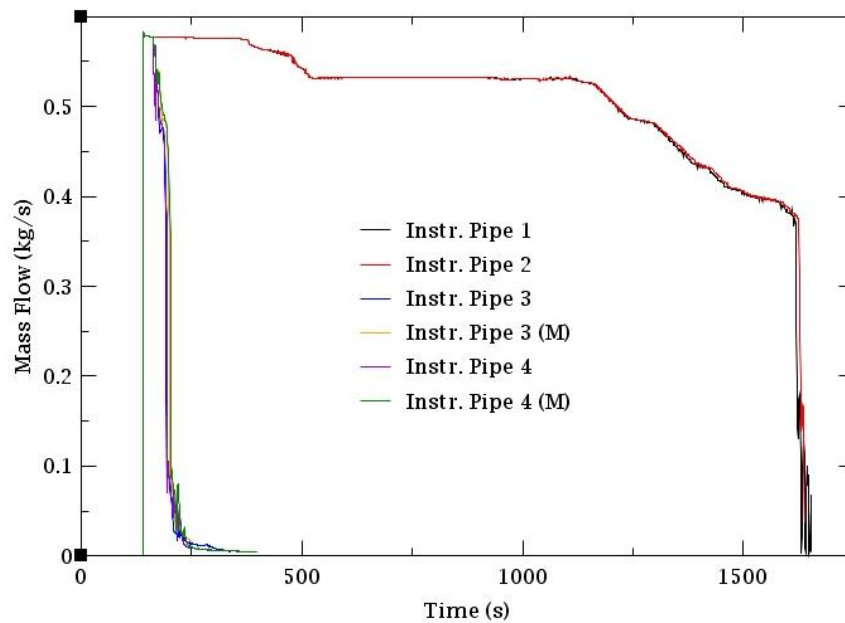


Figure 6.12. Instrumentation Pipe Mass flow rate

Looking at the Figure 2, moreover, at cases 1 and 2, it can be appreciated some clear changing points. Just after the appearance of the break, sodium starts to flow out of KASOLA base loop. The first mass flow rate drop in the graphic, after ~375 seconds, represents that the expansion tank is empty. Afterwards, the mass flow rate remains constant until it starts dropping again progressively from the

second 1100 approx. and drastically around the second 1600, when the basic loop empties down to the level of the break. After this time, the mass flow rate oscillates around the 0.05 kg/s before the simulation stops, as it is shown in the Figure 12:

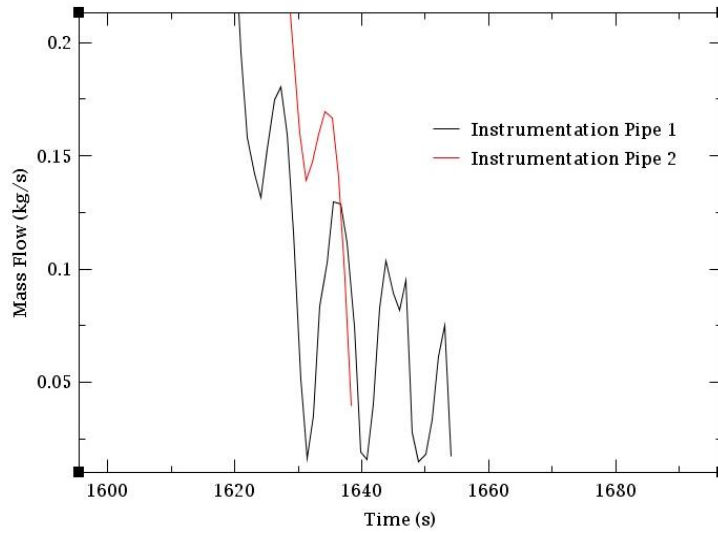


Figure 6.13. Detail of the mass flow rate from cases 1 and 2

Since the cases 1 and 2 take so much time, the rest of the cases cannot be properly appreciated in the graphs. The cases 3 and 4 are also separately shown.

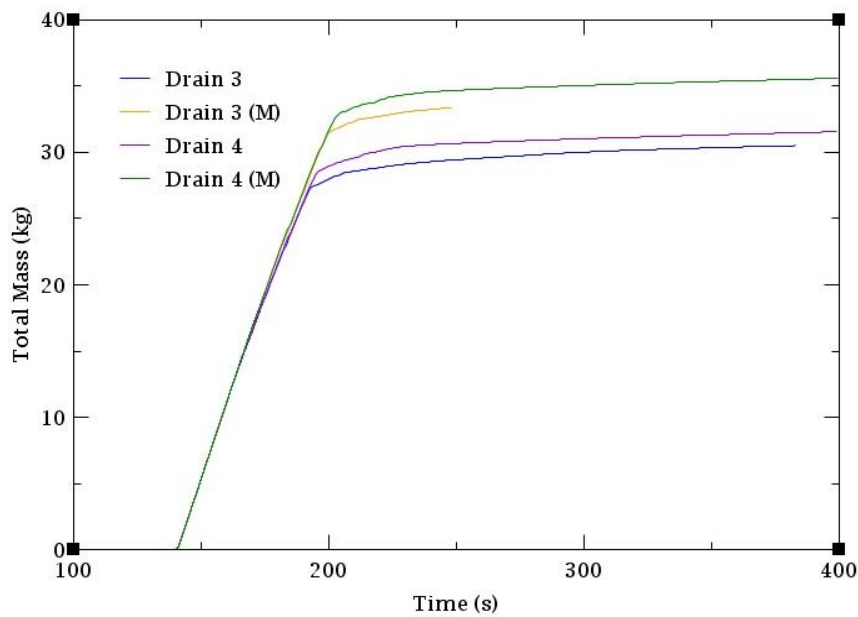


Figure 6.14. Accumulated mass loss for cases 3 and 4

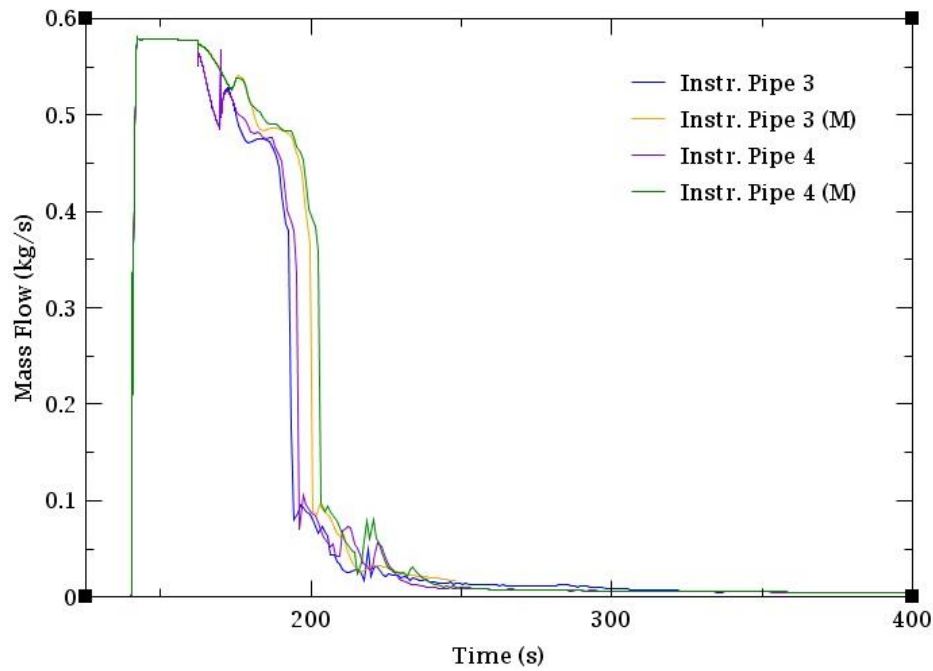


Figure 6.15. Mass flow rate for cases 3 and 4

In cases 3 and 4, after 140 seconds, the break opens, letting sodium flow out of the facility. The mass flow rate remains constant until 160 seconds. At this time, when the fast drain valve starts to open, it can be observed that the mass flow starts to decrease progressively. After 190 seconds, it drops to very low values, what means that there is no more sodium in the basic loop, as everything has been drained into the storage tank. However, some sodium may still remain in the basic loop since the mass flow rate will not stop, as it can be seen in the graphs. Argon gas still flows out of the pipes, and drag some sodium droplets through the brake.

It can also be observed, that the manual simulation of the case 3 ends before than the other cases, after running around 250 seconds. Comparing it to the mass flow rate after the same amount time, it can be seen that it is enough to be analysed.

Scenario	Problem time	Total mass loss	Mass flow rate residuals
Instrumentation Pipe 1	1654,075 s	762.861 kg	0.0045 kg/s
Instrumentation Pipe 2	1638,4 s	765.296 kg	0.037 kg/s

Table 6.10. Mass loss and mass flow rate final values (cases 1 and 2)

Scenario	Problem time	Total mass loss	Mass flow rate residuals
Instrumentation Pipe 3	382.84 s	30,508 kg	0,0047 kg/s
Instrumentation Pipe 3 (M)	248,154 s	33,393 kg	0,017 kg/s
Instrumentation Pipe 4	399.158 s	31,557 kg	0,0048 kg/s
Instrumentation Pipe 4 (M)	399.427 s	35,591 kg	0,0049 kg/s

Table 6.11. Mass loss and mass flow rate final values (cases 3 and 4)

6.4 Large break to the insulation simulation

6.4.2 Transient scenario definition

In order to simulate a more realistic scenario, the insulation surrounding the basic loop should be taken into consideration, since sodium would not flow directly into the atmosphere. For this reason, the behaviour of the fluid through this layer should be studied.

This break scenario is unlikely to happen as the pipe wall is thick and covered by another steel layer but the sensor that detects if a leak is happening is located ~2 metres below the position of the break used in the previous scenarios. For this reason, the sodium flowing through the insulation must be taken into consideration.

Before any research was done, the proposal was to represent the porous media as a pipe with a high wall roughness. After reviewing the literature, it has been found that some approximations have already been done, similar to the initial idea. They come out with different correlations for the friction factor and pressure drop of porous beds for different porosities and flow regimes (R. Byron Bird, 2002). Although this idea was the most promising one, after an empirical study, it has been proved that it cannot be applied in this case.

Hence, a simpler system has been designed. As the material of the insulation, stone wool, has a porosity around $\epsilon = 0.9$ (Carman, 1956), it has been assumed to be empty. Also, the resistance to the flux of sodium through the insulation has not been taken into account. In this simulation, no chemical and thermal interaction is considered between the sodium and the stone wool.

As in the previous scenarios, the same cases will be studied, and the Break will be located at the same point.

Scenario	Valve opening configuration					
	NA-VSR-01		NA-VSR-06		NA-VI-02	
	Initial	Final	Initial	Final	Initial	Final
Porous 1	0 %	0 %	0 %	0 %	0 %	0 %
Porous 2	0 %	0 %	100 %	100 %	100 %	100 %
Porous 3	0 %	100 %	0 %	0 %	0 %	0 %
Porous 3 (M)	0 %	100 %	0 %	0 %	0 %	0 %
Porous 4	0 %	100 %	100 %	100 %	100 %	100 %
Porous 4 (M)	0 %	100 %	100 %	100 %	100 %	100 %

Table 6.12. Valve configuration for each scenario

6.4.3 Improvements over the original KASOLA model

The size of the break will be DN 25, modelled as a valve with that diameter and connected to the basic loop. Since the thickness of the insulation layer is 150 mm, it will be considered as an industrial stainless steel vertical pipe with that same value for the inlet diameter and a length of 2 m. At this height, there is a bend at the basic loop, as shown in figure, where sodium might concentrate. To simulate it, the steel pipe will lead into a small $7 \cdot 10^{-3} m^3$ tank. As it has been said, sodium would leak through the gap left between the overlap of two stainless steel layers. This space will be modelled as a horizontal (with 4 degrees inclination) 1 mm diameter pipe. At the end of the pipe, a break with the outlet boundary conditions is placed. These conditions are also set for the whole break structure. The roughness of every component is $\epsilon = 3.0 \cdot 10^{-5} m$.

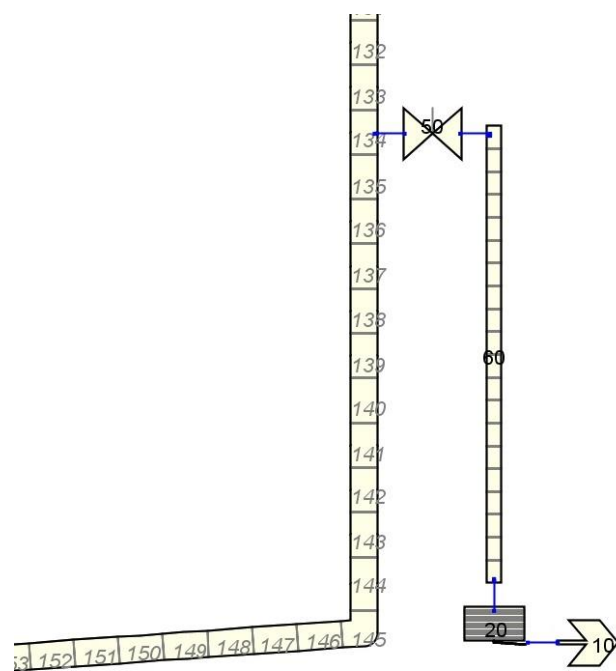


Figure 6.16. Detail of the insulation modeling

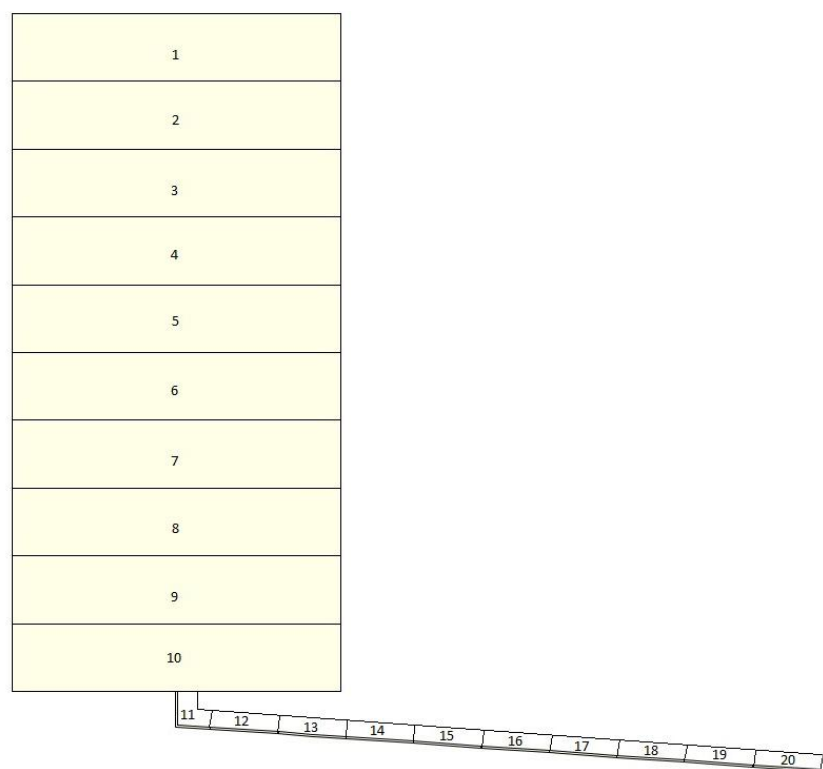


Figure 6.17. Detail of the insulation at the bend modelling

The initial conditions for the whole break structure (*Pipe 60*, *Pipe 20* and *Break 10*), will be the same. The values are shown in the table below.

	Facility	Break structure and atmosphere
Pressure	$1.5 \cdot 10^5 \text{ Pa}$	$1.01 \cdot 10^5 \text{ Pa}$
Gas volume fraction	0.0	1.0

Table 6.13. Model initial conditions

6.4.4 Simulation of the transient and results

In this case, the simulation time for scenarios 1 and 2 will take more time, since the break is really small and the facility empties much slower. An end time of $1.3 \cdot 10^5$ seconds (around 36 hours) has been set, in order to appreciate the results. In the cases 3 and 4, the simulation runs for 10^4 seconds because, even if there is no more sodium in the facility after 200 seconds (*Figure 6.21*), the released coolant takes more time to flow out of the facility. Then, the set timestep data will be the following:

End Time	Minimum Size	Maximum Size	Heat vs Fluid Size Ratio	Max Conv. Power Diff	Long Edit Interval	Graphics Interval	Restart Interval	Short Edit Interval
10.0	1.0E-9	0.1	10.0	1.0E20	10.0	1.0	10.0	10.0
135.0	1.0E-9	0.1	10.0	1.0E20	100.0	1.0	100.0	100.0
175.0	1.0E-9	0.5	10.0	1.0E20	100.0	0.1	100.0	100.0
1.3E5	1.0E-7	0.05	10.0	1.0E20	100.0	10.0	100.0	100.0

Table 6.14. Timestep data table for scenarios 1 and 2

End Time	Minimum Size	Maximum Size	Heat vs Fluid Size Ratio	Max Conv. Power Diff	Long Edit Interval	Graphics Interval	Restart Interval	Short Edit Interval
10.0	1.0E-9	0.1	10.0	1.0E20	10.0	1.0	10.0	10.0
135.0	1.0E-9	0.1	10.0	1.0E20	100.0	1.0	100.0	100.0
175.0	1.0E-9	0.5	10.0	1.0E20	100.0	0.1	100.0	100.0
1.0E4	1.0E-6	0.05	10.0	1.0E20	100.0	5.0	100.0	100.0

Table 6.15. Timestep data table for scenarios 3 and 4

Hence, leaked sodium will be measured at two different points: at the break in the basic loop, in order to see how much flows out of the system into the insulation, and at the gap where it pours into the atmosphere.

After running the simulation for scenarios 1 and 2, it has been seen that the chosen end time is still not enough to see when the sodium stops pouring out of the facility. The case 1 stops after 96923.47 seconds. The results will be observed at

the valve (*Valve 50*) that corresponding to the break of the basic loop, and at the break (*Break 10*) where the sodium leaves the insulation. Afterwards, the total mass of sodium that flows through each component will be compared in order to the extent of seeing how much fluid is contained in the insulation.

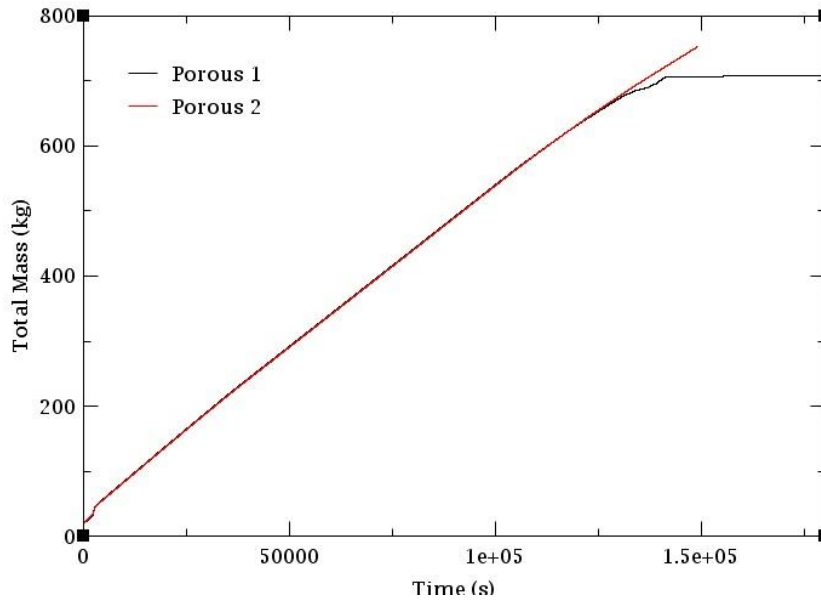


Figure 6.18. Accumulated Sodium mass flow through Valve 50

As the simulation time is really big, in a mass flow rate graph, no change would be appreciated. It has been seen, that after the appearance of the break, the mass flow rate has a value between 0.005 and 0.004 kg/s .

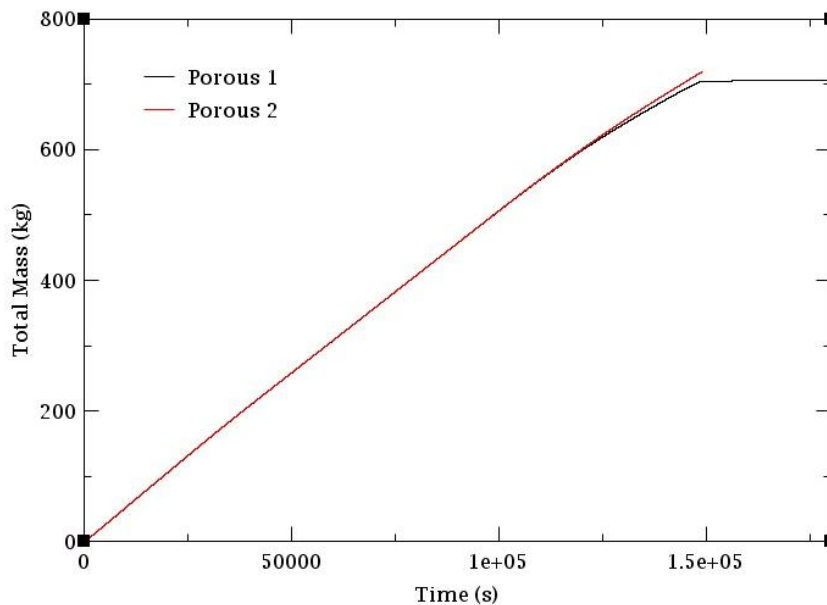


Figure 6.19. Accumulated Sodium mass flow through Break 10

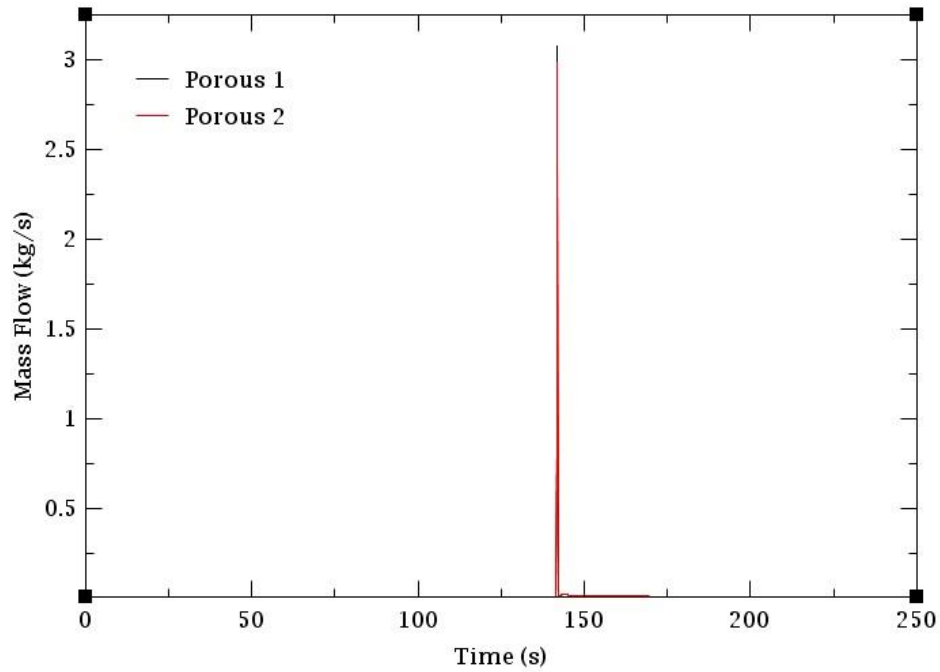


Figure 6.20. Sodium mass flow rate through Break 10

As the initial value for the pressure at the insulation is the atmospheric pressure ($1.01 \cdot 10^5 \text{ Pa}$), as soon as the break appears, there will be an increase in the pressure until the insulation is filled and the first sodium will come at high velocities, as it is shown in the following graph.

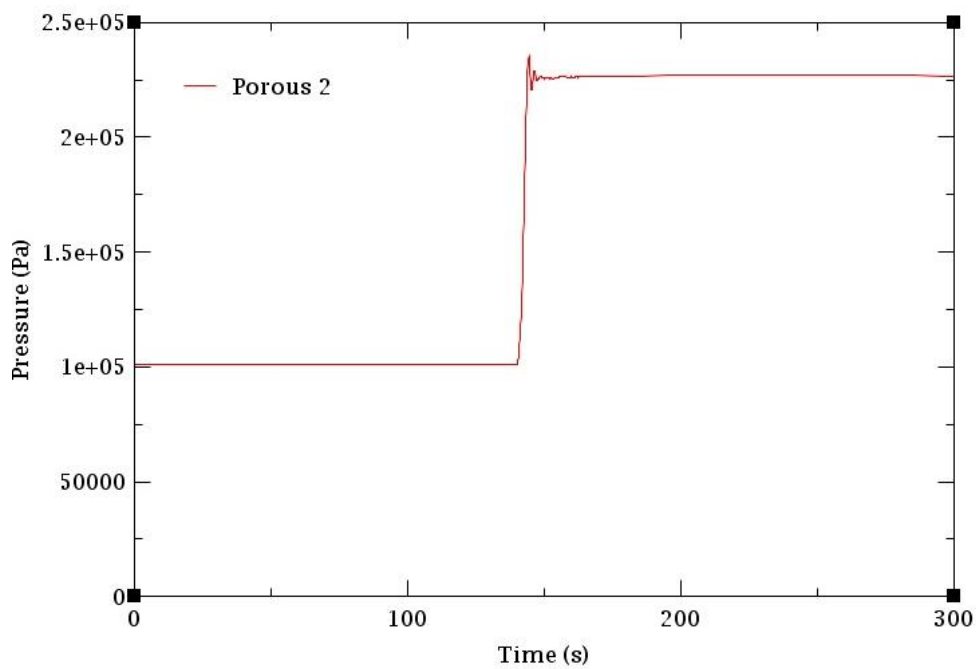


Figure 6.21. Total pressure at the break before and after the valve opens.

The values at the end of the simulation are detailed in the table below.

Scenario	Time	Valve 50	Break 10
Porous 1	96923.47 s	533.375 kg	495.887 kg
Porous 2	129997.08 s	681.306 kg	646.642 kg

Table 6.16. Total sodium mass loss values for cases 1 and 2

At the end times for the first two scenarios, the accumulated sodium at the insulation is 37.488 kg for the first case and 34.664 kg for the second case. In the first case less sodium is lost, because some of it is retained by the hot leg bypass valve and the heat exchanger drain valve.

In cases 3 and 4, sodium is released through the valve in an immediate way, since the break is of great size, and most of it is lost as soon as the hole appears. All the fluid is afterwards contained in the insulation while it slowly pours into the environment, as it can be seen in the figure.

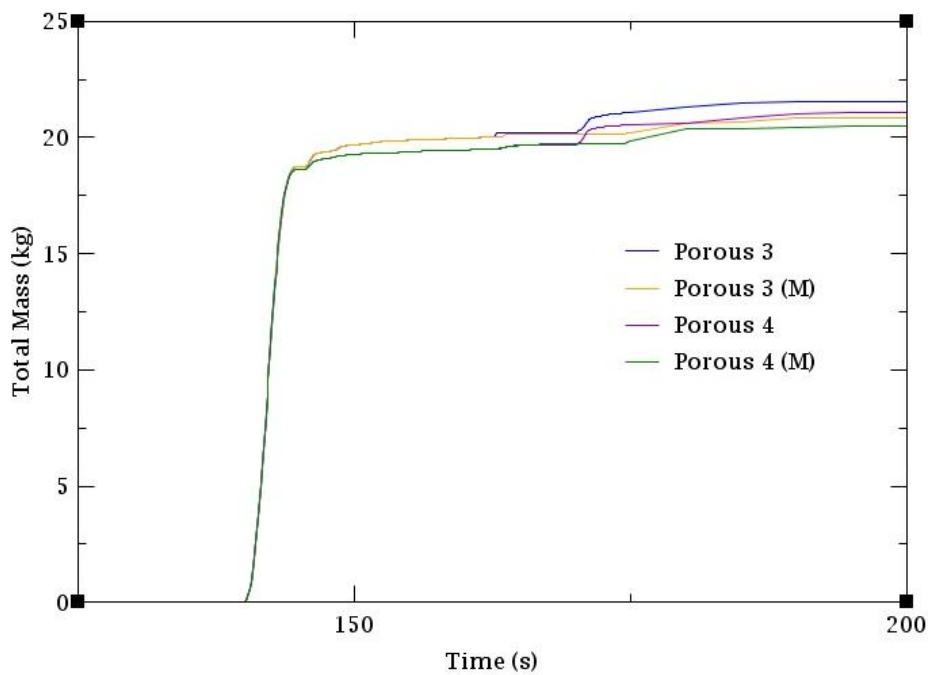


Figure 6.22. Accumulated sodium mass flow through Valve 50 for cases 3 and 4

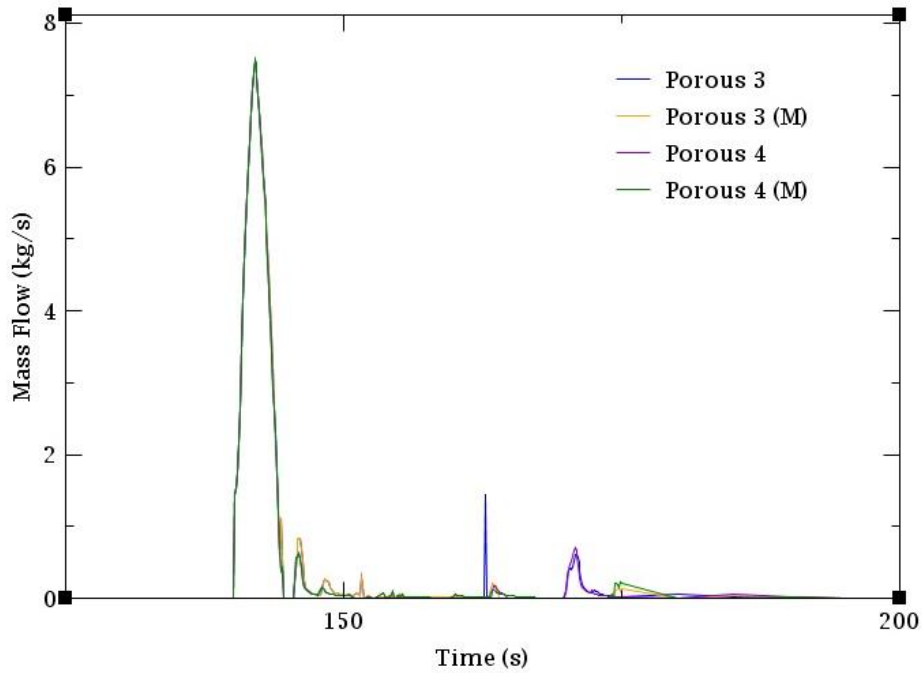


Figure 6.23. Sodium mass flow rate through Valve 50 for cases 3 and 4

Looking at the Figure 16, it can be seen that the sodium is released while there is still some in the facility. Everything is retained in the insulation, and flows into the KASOLA containment at low mass flow rates, as it is shown below.

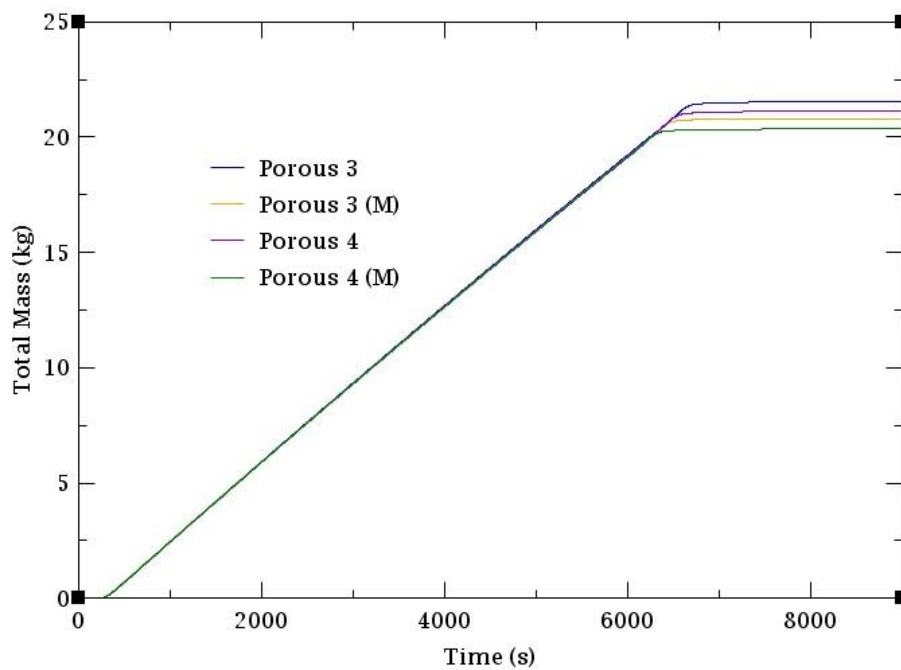


Figure 6.24. Accumulated sodium mass flow through Break 10 for cases 3 and 4

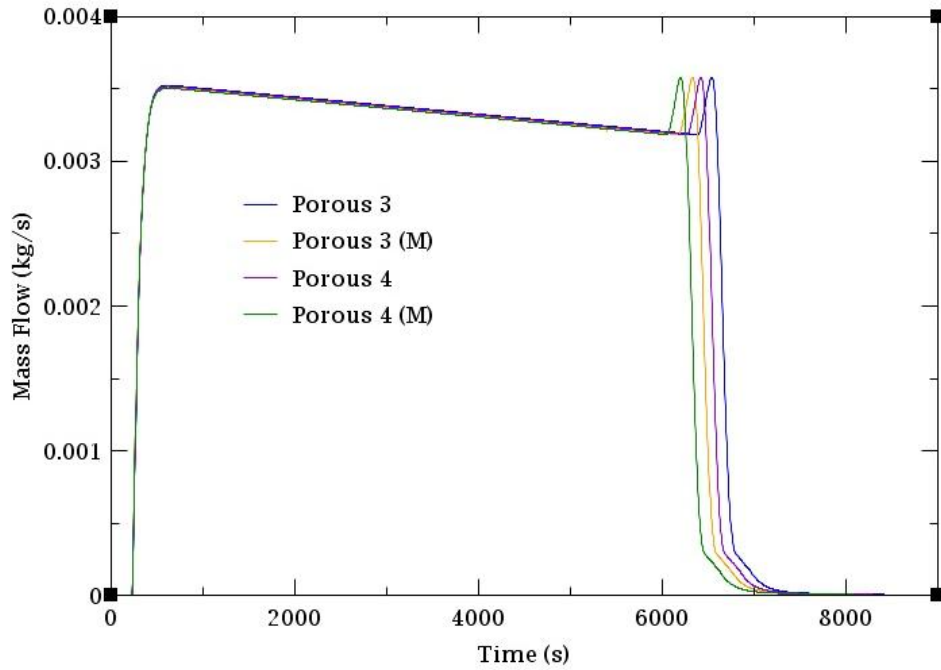


Figure 6.25. Sodium mass flow rate through Break 10 for cases 3 and 4

In the figure below, the peak of the mass flow rate is due to the argon when it starts to flow out the facility. The last drops are pushed by the gas, making the velocity of sodium to slightly increase.

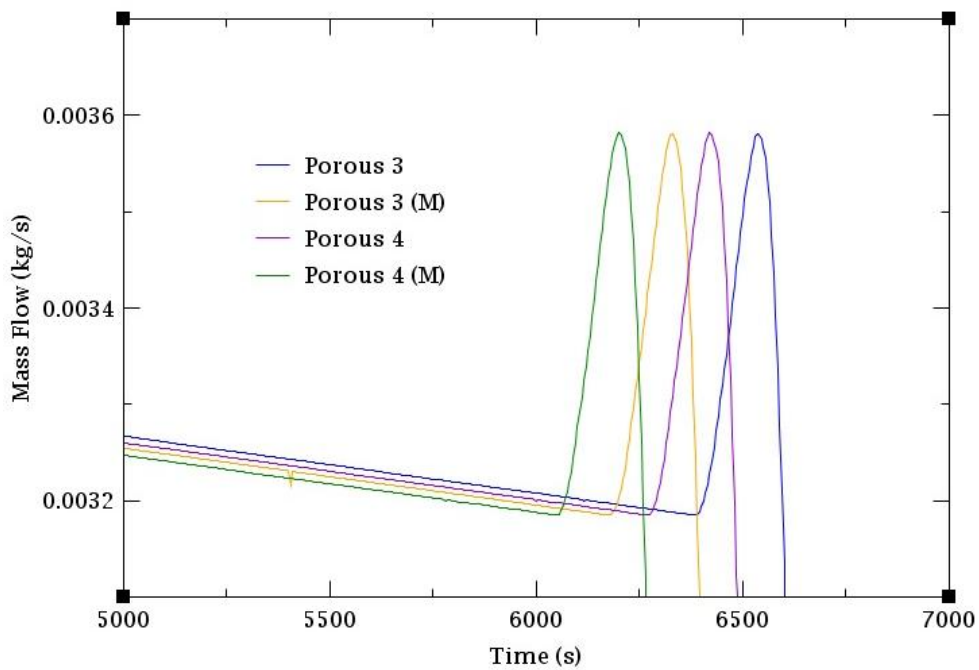


Figure 6.26. Detail of the mass flow rate at 6000 seconds for cases 3 and 4

Looking at the animation of the simulation, the peak shown in Figure 19 coincides with the moment where the small tank is emptied and the last thin pipe releases the remaining sodium.

As it has been said, the area under the mass flow rate curves has been calculated with the integration tool of AptPlot. The results are quite similar for the Valve 50 and the Break 10, as it can be seen in the following table:

Scenario	Valve 50	Break 10
Porous 3	21.565 <i>kg</i>	21.534 <i>kg</i>
Porous 3 (M)	20.868 <i>kg</i>	20.809 <i>kg</i>
Porous 4	21.100 <i>kg</i>	21.123 <i>kg</i>
Porous 4 (M)	20.490 <i>kg</i>	20.538 <i>kg</i>

Table 6.17. Total sodium mass loss values for cases 3 and 4

7 CONCLUSIONS

During the project, an analysis of the development of the KASOLA facility, facing a LOCA type accident, has been done. Three different experiments have been chosen and a total of 18 different cases have been simulated using the thermo-hydraulic TRACE code.

Each simulation corresponds to a different break modelling and, for each test, 6 different scenarios have been taken into account, regarding the valve configuration of the same. The size of the break has been changed as well as the components used for modelling it.

The analysed variables are the sodium mass flow rate, the total mass and the pressure. After the whole process of elaborating this project, and after studying the results, some conclusions have been drawn.

Independently of the simulated experiment, in front of a LOCA, the drainage valve must be immediately opened (if the draining system is not damaged), while the valves at the hot and cold legs are maintained closed, in order to avoid the maximum possible sodium losses.

Difficulties have been found during the process of the obtaining of results, since on several times, the simulation could not reach its end due to convergence failures. Even though the presented results reveal valuable information, potential improvement of the model (like renodalizations or finding a more appropriate timestep data table) may be possible. For this, the presented results are a good base for further projects.

As it has been said in chapter 6.1.3, due to the initial conditions given for the gas argon, in a simulation of the facility, gas would be flowing out of it continuously. This is also an area of improvement

One part of interesting and hard work was the modelling of a system that considered the flow of sodium through the insulation as a porous media. As it has

been said in the chapter 5.3.3, some research has been done and an empirical study has been carried out (shown in the appendix A.2). The investigation seemed promising, as the application of correlations seemed possible. Eventually, a *cul-de-sac* was reached, and no implementation could be done. As a solution, a simpler system was modelled, which gives a general idea of the flow of sodium through the insulation. However, further improvements that consider the porosity of the medium can be done.

In conclusion, even if the used software was not used up to its highest potential, it could be observed its power for modelling and simulating transients in the area of nuclear reactors. Although TRACE is a potent tool, some of its limitations have shown up during the project. But this, in fact, is something that the developers of the code already remark in the TRACE User's guide: "TRACE makes no attempt to capture, in detail, the fluid dynamics in a pipe branch or plenum" (TRACE V5.762 User's Guide Volume 2: Modeling Guidelines). Hence, it is possible that when the simulated problems are reaching their end, the program cannot give accurate results, or converge to a solution. It may be useful to compare the results of the set-into-operation experiments obtained now and in the future with TRACE, with other program, specialized more in the fluid dynamics that may give a more accurate result.

8 PROJECT EXPENSES ESTIMATION

The estimation of the expenses for the accomplishment of this bachelor thesis is done taking into consideration the engineering and project director working hours, the acquisition of software licenses, electronic equipment and other general costs. The cost of the project is illustrative, and calculated as follows:

8.1 Engineering hours

The cost of a mechanical/industrial engineering bachelor is estimated at 15€ per hour. Counting 300 working hours for the realization of the project, according to the UC3M regulation for a bachelor thesis, it results:

$$300 \text{ hours} \cdot 15 \frac{\text{€}}{\text{hours}} = 4500 \text{ €}$$

8.2 Project director

During the realization of the work, an average time of 1 hour per week was spent with the project director. Taking into consideration holidays and cancelled meetings, around 15 hours were spent with the bachelor thesis tutor:

$$100 \frac{\text{€}}{\text{hours}} \cdot 15 \text{ hours} = 1500 \text{ €}$$

8.3 Software license acquisition

The main software used for the execution of this project is the SNAP interface. The remaining computer programs are considered to be totally amortized. Knowing that the United States Nuclear Regulatory Commission does not charge any fee for the code, the technical support and updates are considered. This service costs \$5000 per year, around 4500 €. The time spent at the institute for the development of the project is 4 and a half months. The software cost is:

$$4500 \text{ €} \cdot \frac{5}{12} \text{ months} = 1875 \text{ €}$$

8.4 Electronic equipment

The approximate cost of the electronic equipment (computers, screens...) is 1500€. Since the average useful life of this equipment is 4 years. Since the time spent for the project is 5 months, the electronic equipment cost is:

$$1500 \text{ €} \cdot \frac{5}{48} \text{ months} \cong 160 \text{ €}$$

8.5 General costs

General costs include water and electricity consumption, internet access costs.

$$100 \text{ €}$$

8.6 Summary

Concept	Amount
Engineering hours	4500 €
Project director	1500 €
Software acquisition	1875 €
Electronic equipment	160 €
General costs	100 €
TOTAL	8135 €

REFERENCES

- A. Fritscha, J. F. (2014). Conceptual study of central receiver systems with liquid metals. Beijing: Elsevier.
- Applied Programming Technology, Inc. (2012). *Symbolic Nuclear Analysis Package (SNAP) User's Manual*. Bloomsburg.
- Carman, P. C. (1956). *Flow of Gases Through Porous Media*. London: Butterworths Scientific Publications.
- European Physical Society. (2007). Energy for the future - The Nuclear Option. Mulhouse.
- R. Byron Bird, W. E. (2002). *Transport Phenomena*. New York: John Wiley & Sons.
- U. S. Nuclear Regulatory Commission. *TRACE V5.0 Theory Manual*. Washington, DC.
- U. S. Nuclear Regulatory Commission. *TRACE V5.0 User's Guide Volume 1: Input Specifications*. Washington, DC.
- U. S. Nuclear Regulatory Commission. *TRACE V5.762 User's Guide Volume 2: Modeling Guidelines*. Washington, DC.
- U.S. Nuclear Energy Research Advisory Committee. (2002). *A Technology Roadmap for Generation IV Nuclear Energy Systems*.
- W. Hering, R. S. (2012). Application of liquid metals for solar energy systems. Karlsruhe: EDP Sciences.
- Yoshiaki Oka, K. S. (2008). *Nuclear Reactor Kinetics and Plant Control*. Tokyo: Springer.

APPENDIX

A.1 Results for Drainage simulation of KASOLA with 2 and 3 breaks.

The results obtained for the simulations of KASOLA with two and three breaks will be shown. For each case, the total mass flown through each break will be presented, and the total loss will be calculated. The scenarios with three breaks where the drainage valve is opened, had calculation problems and simulation could not be finished. Hence, only the first two cases will be shown. The tables with the valve configurations will be further on shown.

2 Breaks

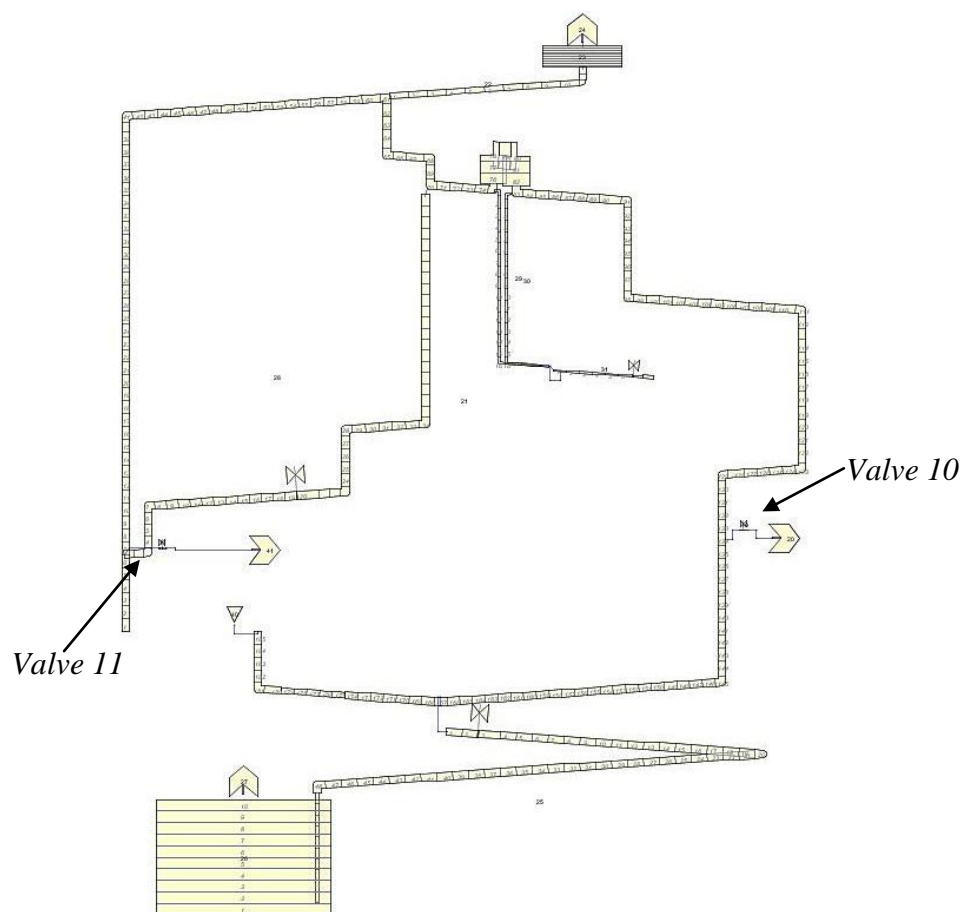


Figure 0.1. KASOLA model with the 2 positions of the breaks

Scenario	Valve opening configuration					
	NA-VSR-01		NA-VSR-06		NA-VI-02	
	Initial	Final	Initial	Final	Initial	Final
Drain 21	0 %	0 %	0 %	0 %	0 %	0 %
Drain 22	0 %	0 %	100 %	100 %	100 %	100 %
Drain 23	0 %	100 %	0 %	0 %	0 %	0 %
Drain 24	0 %	100 %	100 %	100 %	100 %	100 %

Table 0.1. Valve opening configuration for 2 breaks

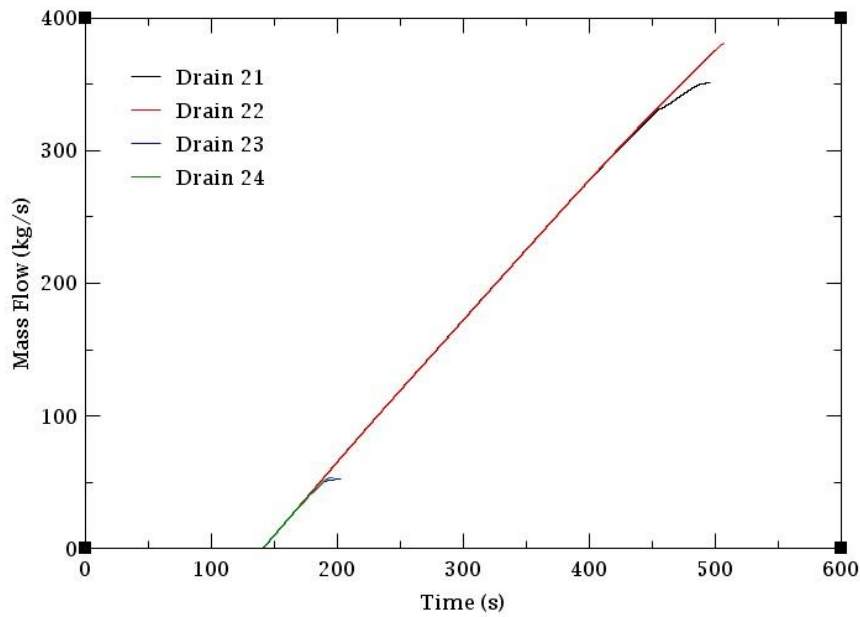


Figure 0.2. Accumulated sodium mass flow through Valve 10

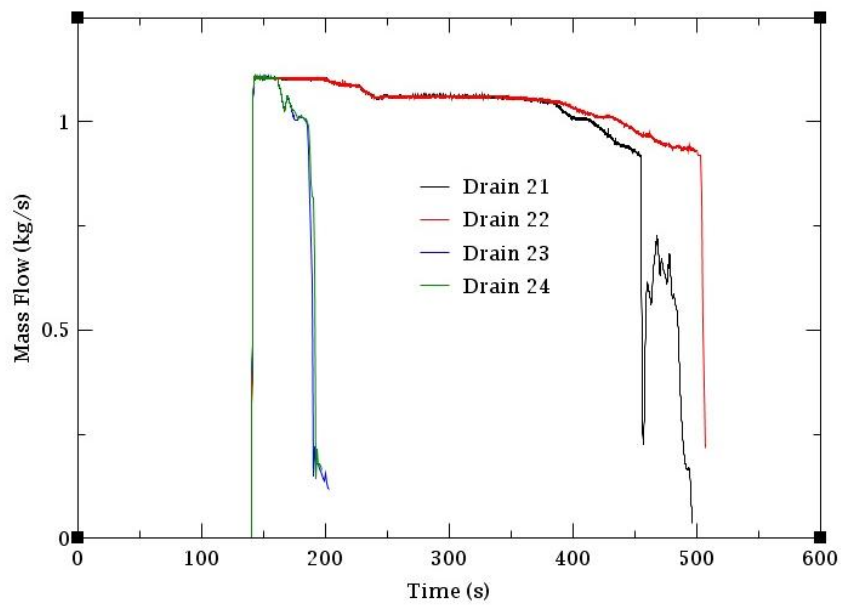


Figure 0.3. Sodium mass flow rate through Valve 10

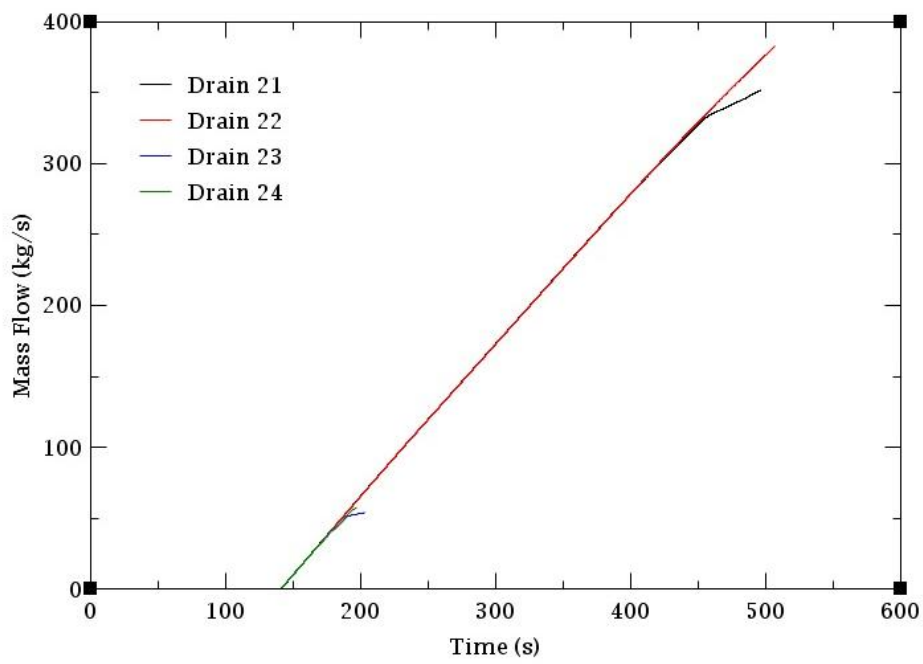


Figure 0.4. Accumulated sodium mass flow through Valve 11

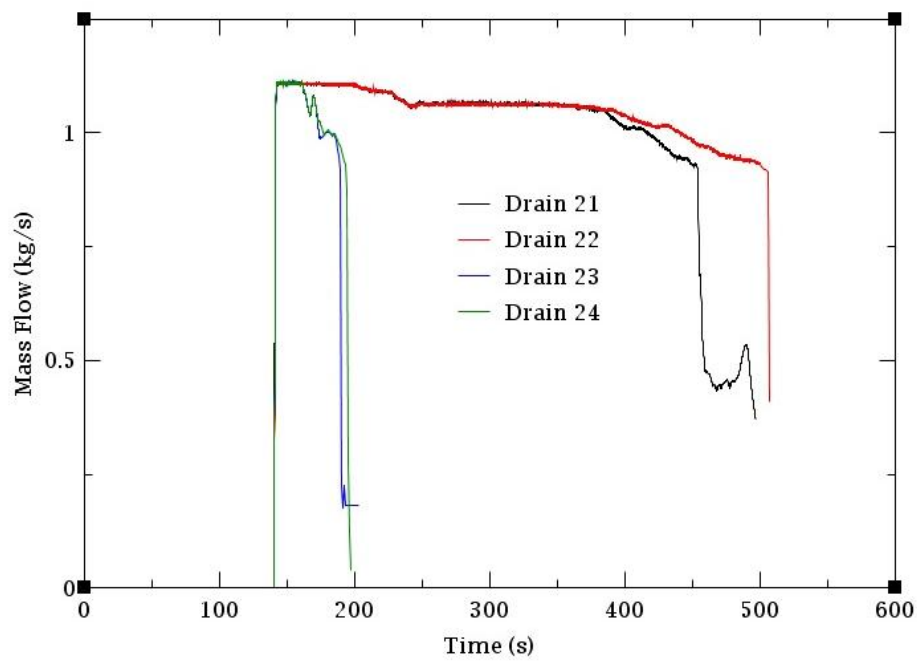


Figure 0.5. Sodium mass flow rate through Valve 11

Scenario	Problem time	Total mass loss
Drain 21	496,646 s	351.378 kg
Drain 22	507.023 s	380.821 kg
Drain 23	203.358 s	52.816 kg
Drain 24	197.288 s	53.747 kg

Table 0.2. Total mass lost through Valve 10

Scenario	Problem time	Total mass loss
Drain 21	496,646 s	351.738 kg
Drain 22	507.023 s	383.143 kg
Drain 23	203.358 s	53.990 kg
Drain 24	197.288 s	56.817 kg

Table 0.3. Total mass lost through Valve 11

Scenario	Problem time	Total mass loss
Drain 21	496,646 s	703.116 kg
Drain 22	507.023 s	763.964 kg
Drain 23	203.358 s	106.806 kg
Drain 24	197.288 s	110.563 kg

Table 0.4. Total mass lost for each scenario

3 Breaks

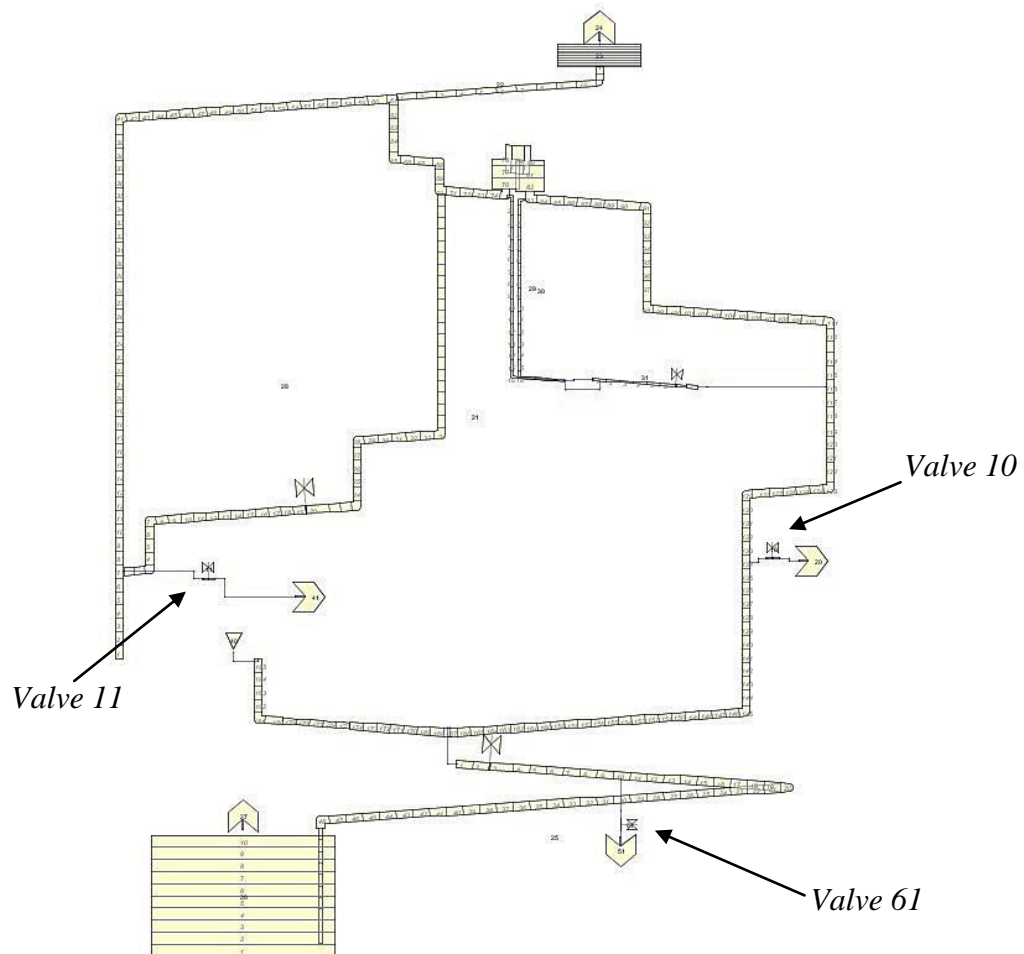


Figure 0.6. KASOLA model with the 3 positions of the breaks

Scenario	Valve opening configuration					
	NA-VSR-01		NA-VSR-06		NA-VI-02	
	Initial	Final	Initial	Final	Initial	Final
Drain 31	0 %	0 %	0 %	0 %	0 %	0 %
Drain 32	0 %	0 %	100 %	100 %	100 %	100 %

Table 0.5. Valve opening configuration for 3 breaks

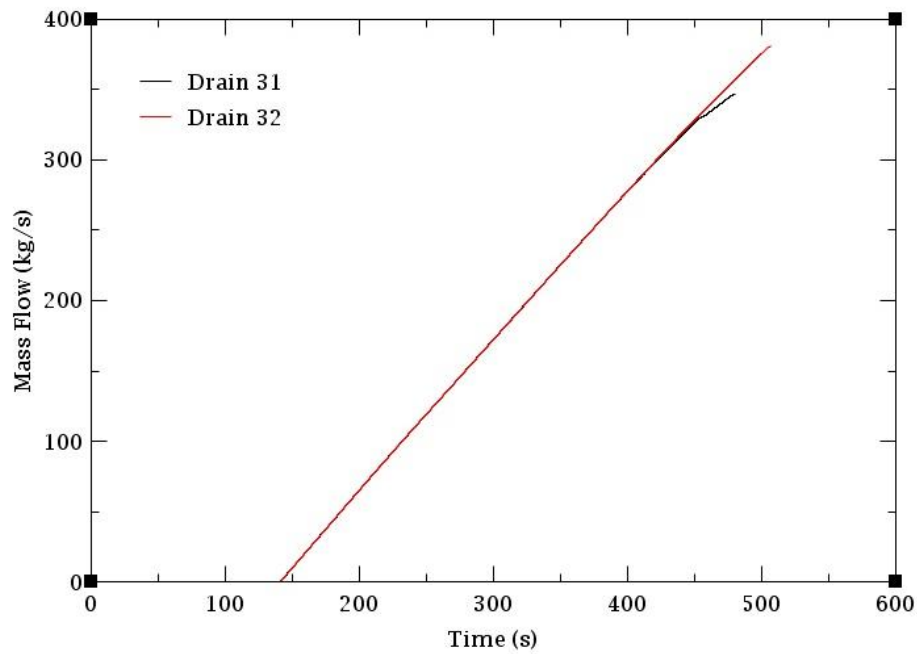


Figure 0.7. . Accumulated sodium mass flow through Valve 10

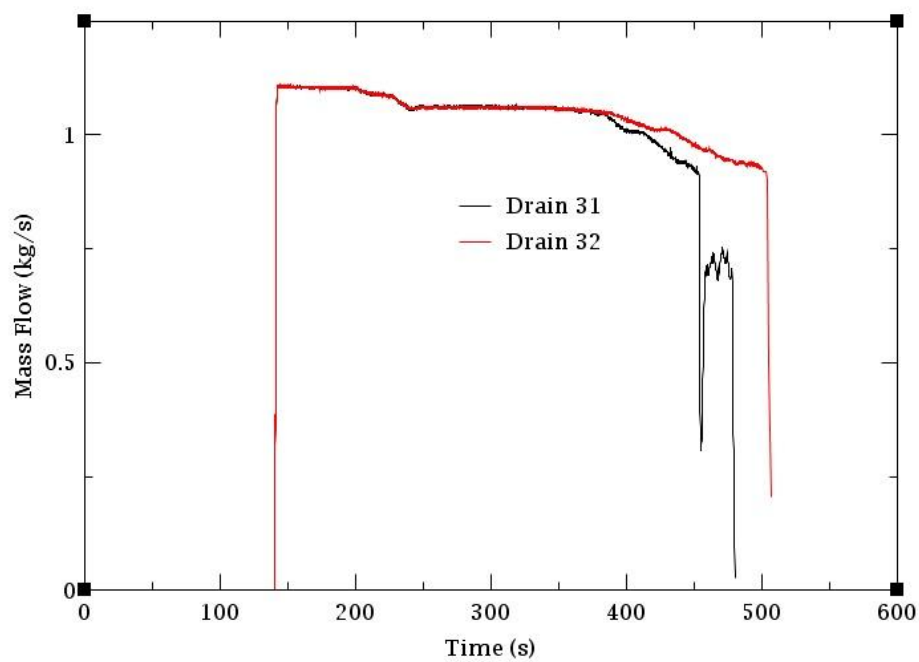


Figure 0.8. Sodium mass flow rate through Valve 10

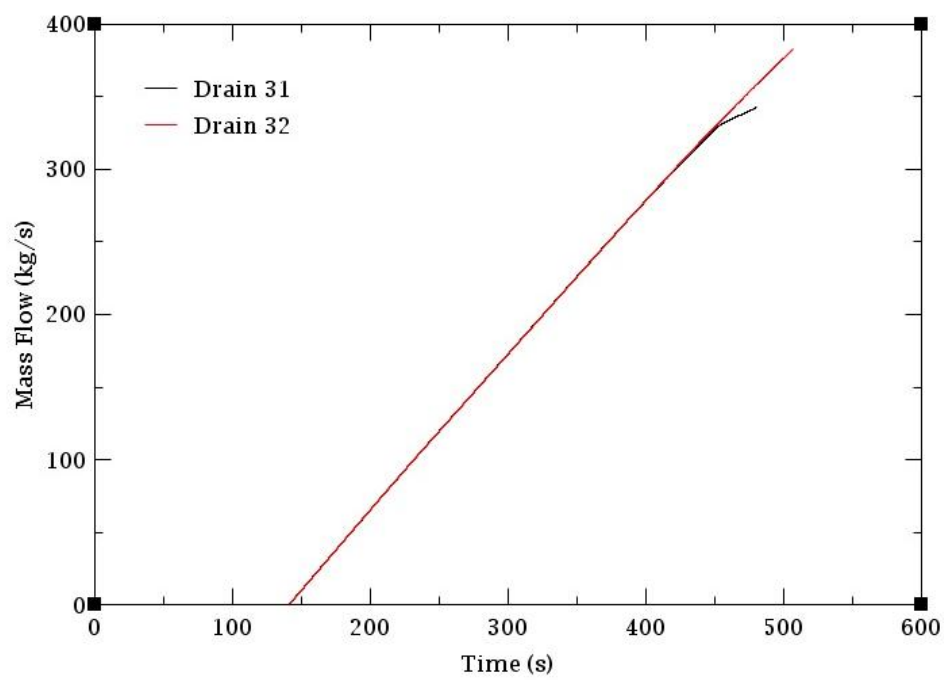


Figure 0.9. Accumulated Sodium mass flow through Valve 11

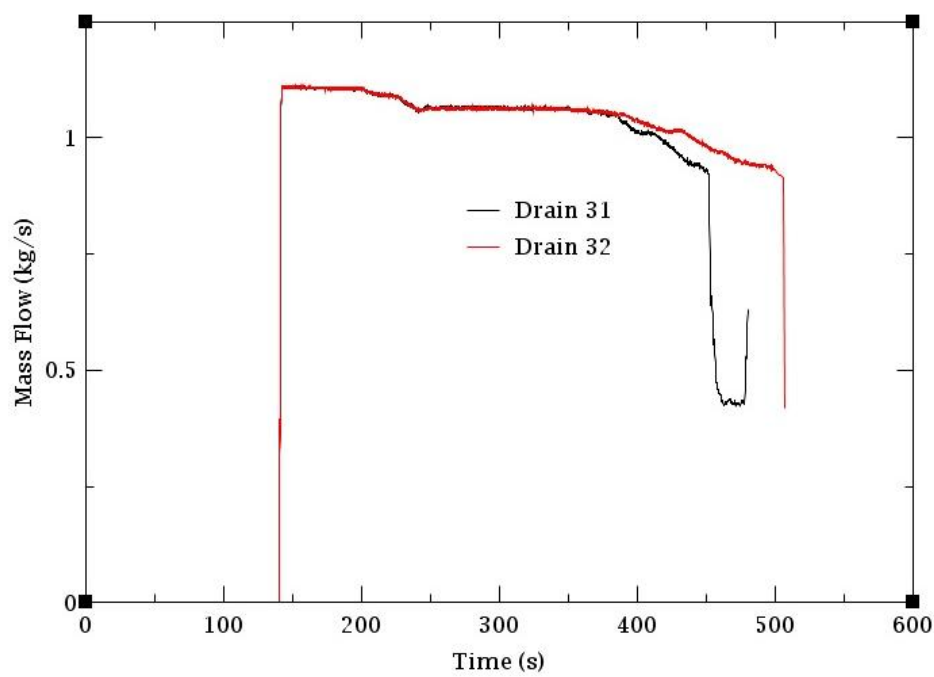


Figure 0.10. Sodium mass flow rate for Valve 11

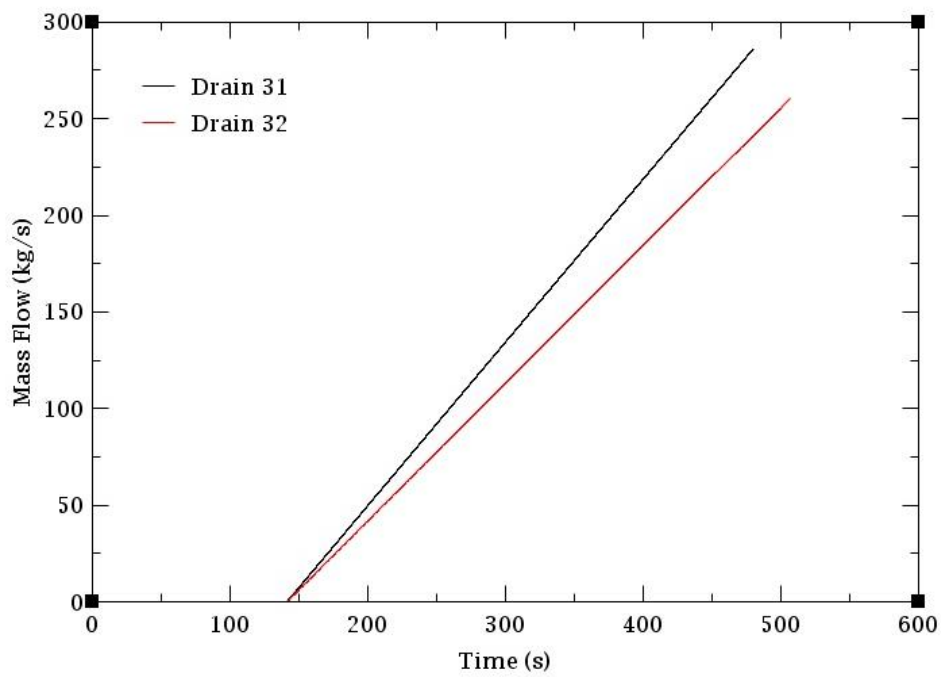


Figure 0.11. Accumulated Sodium mass flow through Valve 61

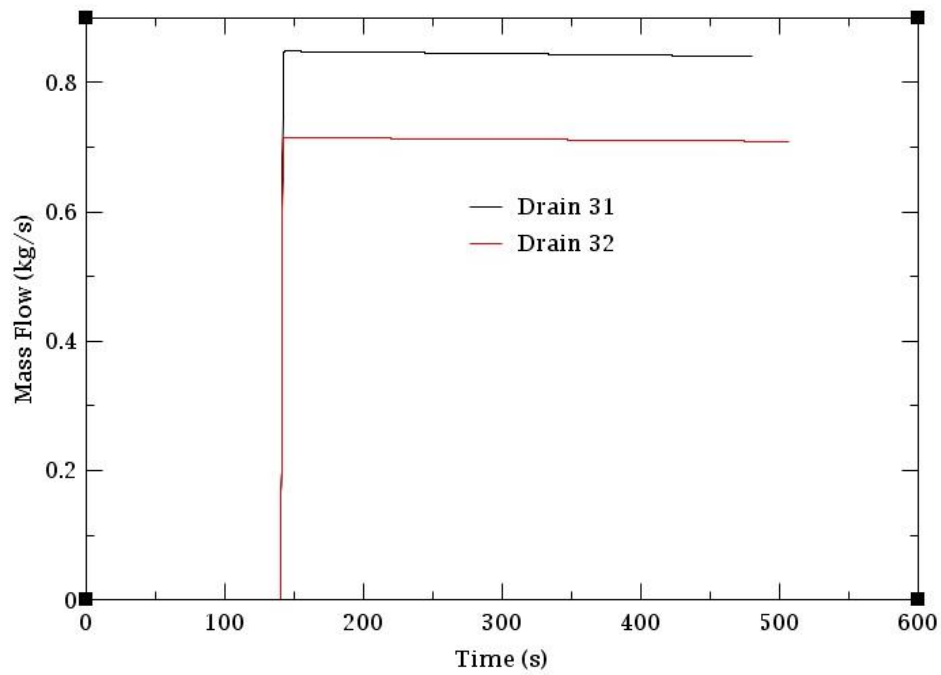


Figure 0.12. Sodium mass flow rate through Valve 61

Scenario	Problem time	Total mass loss
Drain 31	480.2262 s	346.747 kg
Drain 32	507.007 s	380.821 kg

Table 0.6. Total mass lost through Valve 10

Scenario	Problem time	Total mass loss
Drain 31	480.2262 s	342.567 kg
Drain 32	507.007 s	383.128 kg

Table 0.7. Total mass lost through Valve 11

Scenario	Problem time	Total mass loss
Drain 31	480.2262 s	286.175 kg
Drain 32	507.007 s	260.395 kg

Table 0.8. Total mass lost through Valve 61

Scenario	Problem time	Total mass loss
Drain 31	480.2262 s	975.489 kg
Drain 32	507.007 s	1024.392 kg

Table 0.9. Total mass lost for each scenario

In the case of three breaks, the studies must be developed. Even if there is a break after the drainage valve, it cannot be possible that, when it is closed, there is on the piping more than 250 kg of sodium.

A.2 Empirical study on the application of correlations for fluxes through porous media.

The study of the flow of liquids through the micro channels of the porous material is extremely complicated and it could not be possible to analyse until Henry Philibert Gaspard Darcy proposed his statement. The Darcy law says that the flow velocity is proportional to the pressure drop.

$$u = -\frac{B_0}{\mu} \cdot \frac{\Delta p}{L} \quad (1)$$

Where B_0 is the permeability coefficient of the porous media.

Although progress has been done in the study of this area, correlation methods are the most used, which are based in the relation of the pressure loss with the friction of the fluid with the material. One approximation consists on relating it with the flux of the fluid through a column full of spheres but, indeed, the most common is to relate the porous media to a channel bundle which have an irregular cross section rather. This approach may be acceptable, as what is intended to study, to represent, is the macroscopic flux of the sodium through the stone wool. For this specific case is useful, since what is intended to obtain is an equivalent friction factor for the porous material.

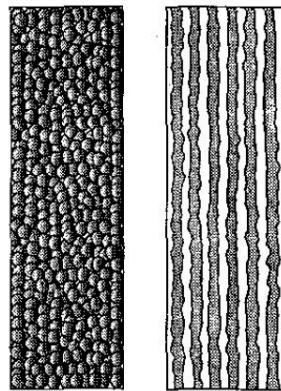


Figure 0.13. Cylindrical tube full with spheres (left) and model of a channel bundle (right)

The isolation material, as said, it is stone wool, and from different bibliography, it has been found that it has a porosity around $\varepsilon = 0.9$.

Some studies have already been carried out, where correlations for the friction factor of a porous material were obtained. These correlations differ between them since they take into consideration different porosities and flow regimes. Usually, they work with lower and medium values and, thus, a friction factor for higher porosities shall be estimated from them.

For laminar flow, the Blake-Kozeny equation has in general good results, as soon as the porosity is less than $\varepsilon = 0.5$.

$$\zeta_{channel} = \frac{100}{3 \cdot Re} \quad (2)$$

Where Re is the Reynolds number.

When there is a transition flow, $10 < Re_p < 1000$, Ergun proposes that for porosities between $\varepsilon = 0.55$ and $\varepsilon = 0.75$, the friction factor correlation has the following form:

$$\zeta_{channel} = \frac{2}{3} \cdot \left(\frac{\varepsilon^3}{1 - \varepsilon} \right) \cdot \left(1.75 + \frac{150 \cdot (1 - \varepsilon)}{Re} \right) \quad (3)$$

In turbulent flows, the Burke-Plummer equation will be used, which, however is independent of the Reynolds number. This correlation is valid for low porosities.

$$\zeta_{channel} = \frac{7}{12} \quad (4)$$

These three correlations are used to calculate the pressure drop at the channels, as it is shown all together with some experimental data in the figure 5.2-1.

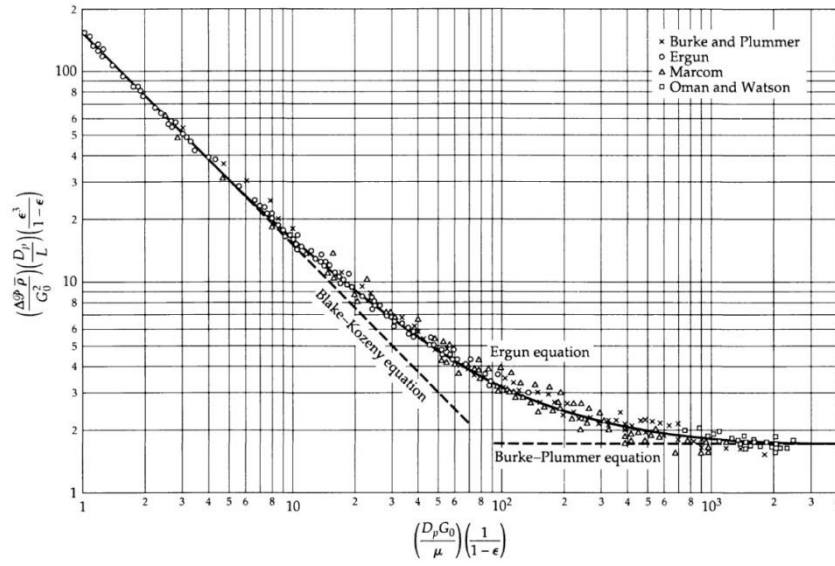


Figure 0.14. Ergun equation and the two asymptotes related to the Blake-Kozeny and Burke-Plummer equations

This figure shows for which flow regime is each equation more appropriate. However, we want to get a relation between the porosity of the material and the friction factor for different Reynolds numbers. The idea is to combine solutions for different cases in order to obtain correlations for the calculation of the friction factor at high porosities. This has been done for the values of the Reynolds number: 1, 10, 100 and 1000.

- **$Re = 1$** : In this case, the correlations of Blake-Kozeny and Ergun have been used. The first one for porosities lower than 0.55 and the second one for those which are higher. Plotting the data and adding a trend line shows that the best type of equation that better fits the points is the polynomial one. Subsequently, the following correlation is obtained:

$$\zeta = 772.99 \cdot \varepsilon^2 - 978.67 \cdot \varepsilon + 342.64 \quad (5)$$

As the porosity of the stone wool is $\varepsilon = 0.9$, the estimated value of the friction factor for $Re = 1$ is:

$$\zeta = 87.959 \quad (6)$$

- **$Re = 10$** : The correlations of Blake-Kozeny and Ergun have been also used for this case and a trending line of the polynomial type seems also to be the most appropriate. The correlation in this case is the following:

$$\zeta = 86.96 \cdot \varepsilon^2 - 97.721 \cdot \varepsilon + 30.582 \quad (7)$$

Giving a value for the friction factor of:

$$\zeta = 13.071 \quad (8)$$

- **$Re = 100$** : In this case, the Blake-Kozeny correlation has been substituted by the Burke-Plummer correlation, as it is more appropriate for higher flow regimes through lower porosities. For the medium porosities, the Ergun correlation is still used. The correlation function is the following:

$$\zeta = 34.628 \cdot \varepsilon^2 - 35.422 \cdot \varepsilon + 9.5786 \quad (9)$$

Leading to a friction factor of

$$\zeta = 5.747 \quad (10)$$

- **$Re = 1000$** : Again, the Blake-Plummer correlation is used for the lower porosities and the Ergun correlation for the medium ones. The correlation for the friction factor resulting from the other two correlations is:

$$\zeta = 33.609 \cdot \varepsilon^2 - 35.591 \cdot \varepsilon + 9.8948 \quad (11)$$

And, thus, the value of the friction factor for the porosity of the stone wool is

$$\zeta = 5.086 \quad (12)$$

Therefore, we have four values of the friction factor at different flow regimes for a porosity of $\varepsilon = 0.9$.

Re	ζ
1	87,959
10	13,071
100	5,747
1000	5,086

Table 0.10. Obtained values for the friction factor

The TRACE code uses the Churchill correlation for the calculation of the friction factor as a function of the Reynolds number, the hydraulic diameter D and the

roughness ϵ . As the friction factor has been already estimated, a correlation for ϵ/D will be obtained from the initial one. The Churchill equation is the following:

$$\zeta = \left[\left(\frac{8}{Re} \right)^{12} + \frac{1}{(A+B)^{3/2}} \right]^{1/12} \quad (13)$$

where

$$A = \left[2.457 \cdot \ln \frac{1}{\left(\frac{7}{Re} \right)^{0.9} + \frac{0.27\epsilon}{D}} \right]^{16} \quad (14)$$

$$B = \left(\frac{37530}{Re} \right)^{16} \quad (15)$$

Valid for any Re and ϵ/D . By doing basic operations, ϵ/D is left out in the following way:

$$\frac{\epsilon}{D} = \frac{1}{0.27} \left[e^{-\left(\frac{1}{2.457} (C-D)^{-16} \right)} - \left(\frac{7}{Re} \right)^{0.9} \right] \quad (16)$$

Where

$$C = \left[\zeta^2 - \left(\frac{8}{Re} \right)^{12} \right]^{-8} \quad (17)$$

$$D = \left(\frac{37530}{Re} \right)^{16} \quad (18)$$

From this, one correlation is obtained for each Reynolds number. However, for the obtained values it is impossible to calculate, since in certain point, a negative square root appears.

The last correlation shall be modified, in order that the component of equation (13) shown in the equation (19) is satisfied.

$$\left[\left(\left(\frac{\zeta}{2} \right)^{12} - \left(\frac{8}{Re} \right)^{12} \right)^{-\frac{2}{3}} - \left(\frac{37530}{Re} \right) \right] > 0 \quad (19)$$

The correlation corresponding to $Re = 1000$ will be modified for higher Reynolds numbers, starting with the value for $\zeta = 5.086$.

At the end, $\zeta = 5.01214$ and $Re = 5.83881 \cdot 10^7$ are obtained. If these values are introduced in the equation (13), the final result, which is not possible to follow, is shown below.

$$\frac{\epsilon}{D} = -0.000675 \quad (20)$$

To conclude, although no more calculations have been done in this direction, the first obtained results of the study show that this technique cannot be implemented for the case of the insulation of the facility.